CNN Pincer Ruthenium Catalysts for Hydrogenation and Transfer Hydrogenation of Ketones: Experimental and Computational Studies

11 AUTHORS, INCLUDING:

Walter Baratta
University of Udine
86 PUBLICATIONS   **2,241** CITATIONS

SEE PROFILE

Paulo Jorge Costa
University of Aveiro
63 PUBLICATIONS   **1,150** CITATIONS

SEE PROFILE

Carlo Mealli
Italian National Research Council
245 PUBLICATIONS   **5,039** CITATIONS

SEE PROFILE

Abdelatif Messaoudi
The University of Batna
17 PUBLICATIONS   **148** CITATIONS

SEE PROFILE

‖**Hydrogenation** |*Very Important Paper*|

CNN Pincer Ruthenium Catalysts for Hydrogenation and Transfer Hydrogenation of Ketones: Experimental and Computational Studies

Walter Baratta,*[a] Salvatore Baldino,[a] Maria José Calhorda,[b] Paulo J. Costa,[c] Gennaro Esposito,[d] Eberhardt Herdtweck,[e] Santo Magnolia,[a] Carlo Mealli,[f] Abdelatif Messaoudi,[f] Sax A. Mason,[g] and Luis F. Veiros[h]

Abstract: Reaction of [RuCl(CNN)(dppb)] (**1-Cl**) (HCNN = 2-aminomethyl-6-(4-methylphenyl)pyridine; dppb = Ph_2P-$(CH_2)_4PPh_2$) with $NaOCH_2CF_3$ leads to the amine-alkoxide [Ru-(CNN)(OCH₂CF₃)(dppb)] (**1-OCH₂CF₃**), whose neutron diffraction study reveals a short RuO···HN bond length. Treatment of **1-Cl** with NaOEt and EtOH affords the alkoxide [Ru(CNN)-(OEt)(dppb)]·(EtOH)$_n$ (**1-OEt·nEtOH**), which equilibrates with the hydride [RuH(CNN)(dppb)] (**1-H**) and acetaldehyde. Compound **1-OEt·nEtOH** reacts reversibly with H_2 leading to **1-H** and EtOH through dihydrogen splitting. NMR spectroscopic studies on **1-OEt·nEtOH** and **1-H** reveal hydrogen bond interactions and exchange processes. The chloride **1-Cl** catalyzes the hydrogenation (5 atm of H_2) of ketones to alcohols (turnover frequency (TOF) up to $6.5 \times 10^4\,h^{-1}$, 40 °C). DFT calculations were performed on the reaction of [RuH(CNN′)-(dmpb)] (**2-H**) (HCNN′ = 2-aminomethyl-6-(phenyl)pyridine; dmpb = $Me_2P(CH_2)_4PMe_2$) with acetone and with one molecule of 2-propanol, in alcohol, with the alkoxide complex being the most stable species. In the first step, the Ru-hydride transfers one hydrogen atom to the carbon of the ketone, whereas the second hydrogen transfer from NH_2 is mediated by the alcohol and leads to the key "amide" intermediate. Regeneration of the hydride complex may occur by reaction with 2-propanol or with H_2; both pathways have low barriers and are alcohol assisted.

Introduction

The catalytic hydrogenation (HY)[1] and transfer hydrogenation (TH)[2] of ketones and aldehydes are core processes for the synthesis of alcohols. A subject of current academic and industrial relevance is the asymmetric reduction of prochiral ketones promoted by transition-metal complexes displaying well-designed chiral ligands. Among the numerous systems, those based on Rh, Ir, and Ru have successfully been used in the TH and HY reactions, even though Os also has recently exhibited a similarly good potential.[3] As shown in Scheme 1, the HY process occurs with the reduction of the C=O group by molecular hydrogen (top), whereas TH involves two H atoms provided by a hydrogen donor molecule (bottom), such as 2-propanol.[4]

[a] Prof. W. Baratta, Dr. S. Baldino, Dr. S. Magnolia
Dipartimento di Chimica, Fisica e Ambiente
Università di Udine, Via Cotonificio 108
33100 Udine (Italy)
Fax: (+39) 0432-558803
E-mail: walter.baratta@uniud.it

[b] Prof. M. J. Calhorda
Departamento de Química e Bioquímica
CQB, Faculdade de Ciências
Universidade de Lisboa, Campo Grande
1749-016 Lisboa (Portugal)

[c] Dr. P. J. Costa
Departamento de Química
QOPNA and Secção Autónoma de Ciências
da Saúde Universidade de Aveiro, 3810-193 Aveiro (Portugal)

[d] Prof. G. Esposito
Dipartimento di Scienze Mediche e Biologiche
Università di Udine, P.le Kolbe 4
I-33100 Udine (Italy)

Current Address:
Science & Math Division
New York University Abu Dhabi
Abu Dhabi (UAE)

[e] Dr. E. Herdtweck
Anorganisch-chemisches Institut
Technische Universität München
Lichtenbergstrasse 4, D-85747 Garching (Germany)

[f] Dr. C. Mealli, Dr. A. Messaoudi
Istituto di Chimica dei Composti
Organometallici (ICCOM-CNR),
Via Madonna del Piano, I-50019 Sesto Fiorentino (Italy)

[g] Dr. S. A. Mason
Institut Max von Laue - Paul Langevin
6, Rue Jules Horowitz, BP 156, 38042, Grenoble Cedex 9 (France)

[h] Prof. L. F. Veiros
Centro de Química Estrutural, Complexo I, Instituto Superior Técnico
Universidade de Lisboa, Avenida Rovisco Pais
1049-001 Lisboa (Portugal)

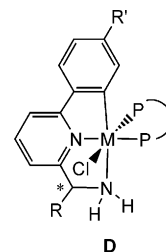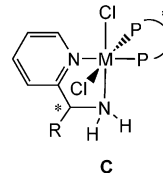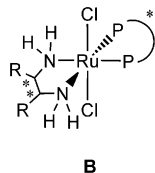Supporting information for this article is available on the WWW under
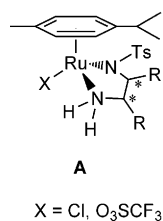http://dx.doi.org/10.1002/chem.201402229.
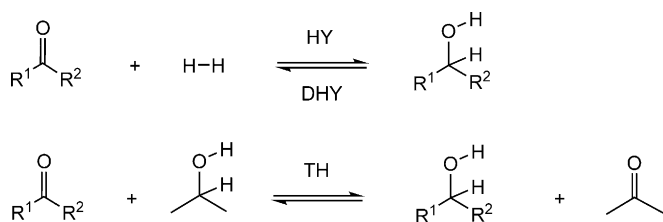
Scheme 1. Hydrogenation (HY) and transfer hydrogenation (TH) reactions.

In principle, HY is thermodynamically more favorable than TH and leads to complete reduction of the starting ketone at low temperature. On heating, the alcohol undergoes the reverse catalytic process, namely the dehydrogenation (DHY) with formation of ketones and H_2.[5] TH with 2-propanol is an equilibrium reaction that can be shifted to the desired alcohol product by performing the reaction in 2-propanol as a solvent. Because of its operational simplicity, mild methodology, and absence of the risks associated with the use of H_2, the use of TH is becoming increasingly common in industrial plants and can be competitive with respect to HY. In both catalytic TH and HY reactions, a metal-hydride species,[6] usually generated from a chloride precursor, is the key intermediate that reacts with the carbonyl substrate leading to a metal-alkoxide complex through a migratory insertion reaction (Scheme 2).[7]

In the "inner-sphere TH mechanism", the M−H species is regenerated from the metal alkoxide upon reaction with 2-propanol to afford the metal-isopropoxide, which undergoes a β-hydrogen elimination reaction (upper part of Scheme 2). Conversely, in the HY, the metal-alkoxide reacts with H_2, possibly involving a M-η^2-H_2 complex,[8] with formation of the M−H bond through a H-H splitting (lower part of Scheme 2). Notably, the metal-alkoxide C−H-activation generally requires a *cis* vacant site,[9] although a facile β-hydrogen elimination in 18-electron Ir^{III} complexes has been claimed by Milstein and Blum.[10]
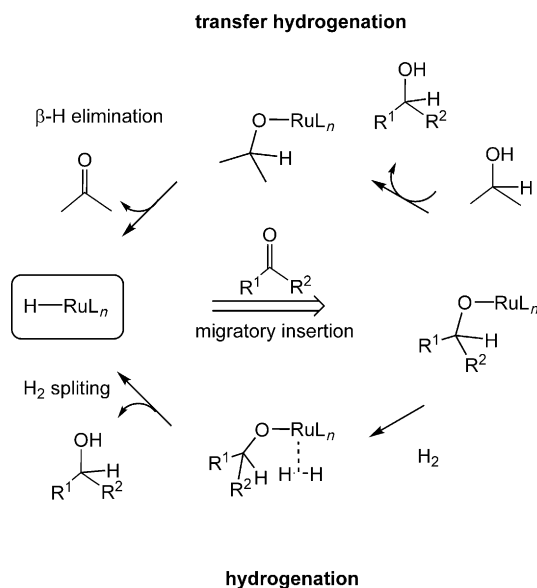
A breakthrough in asymmetric TH and HY is due to Noyori and co-workers with the development of the systems [(η^6-arene)RuCl(Tsdpen)][11] (**A**) (Tsdpen = TsNCHPhCHPhNH₂, Ts = $SO_2C_6H_4CH_3$) and *trans*-[RuCl₂(PP)(1,2-diamine)][12] (PP = BINAP)[13] (**B**), each of them favoring one type of catalysis (Figure 1).

This fundamental work has led to the development of an extensive number of catalysts giving a broad scope for both processes.[1,2] The high activity of these systems is attributed to the NH_2 functionality, which is crucial for the formation of 16-electron Ru-amide species. In the TH mechanism of the Ru(η^6-arene) system (**A**), involving the formation of a metal-hydride intermediate, the adjacent Ru−H/Ru−NH_2 linkages react with the substrate leading to the alcohol product and the Ru-amide,

Scheme 2. Reduction of carbonyl compounds through the inner-sphere TH and HY pathway.

Scheme 3. Reduction of carbonyl compounds through the outer-sphere TH and HY pathway.

X = Cl, O₃SCF₃
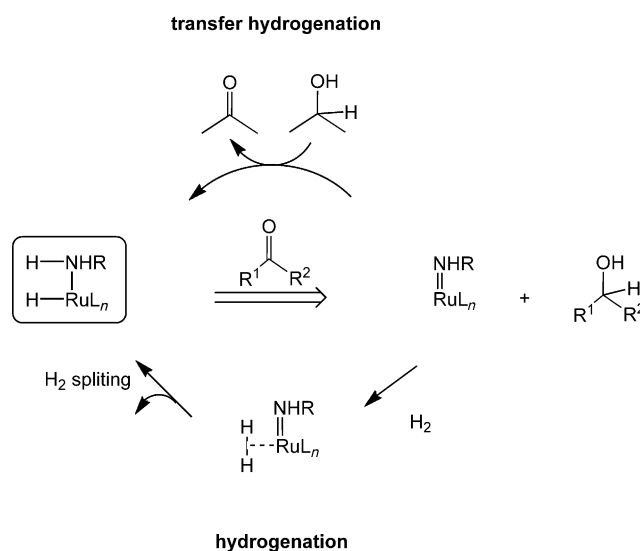
M = Ru, Os

Figure 1. Highly efficient Ru and Os catalysts for asymmetric transfer hydrogenation and hydrogenation of ketones.

which was characterized in the solid state and exhibits a Ru—N double bond (Scheme 3).[11]

The RuH/—NH$_2$ complex is then regenerated by reaction of the Ru-amide with 2-propanol (upper part of Scheme 3). This pathway has been substantiated by DFT calculations, which suggest a concerted delivery of C—H and O—H hydrogen atoms from 2-propanol to the Ru-amide through an outer-sphere mechanism (metal–ligand bifunctional catalysis).[14] In addition, the calculations show that reaction of the Ru-amide with alcohol leads to the 18-electron alkoxide amine complex [(η^6-arene)Ru(OR)(Tsdpen)], which has been regarded as a catalytic reservoir.[14a] Although the latter could not be isolated, Ikariya and Koike reported the formation of the alkoxide [(η^6-arene)Ru(OCH$_2$CF$_3$)(Tsdpen)] at low temperature.[15] Concerning [RuCl$_2$(PP)(1,2-diamine)] (**B**), which is better suited for HY, treatment of the double hydride intermediate [Ru(H)$_2$(PP)(1,2-diamine)] with the substrate affords the alcohol product and the Ru-amide, as validated by theoretical calculations by the groups of Andersson,[16] Noyori,[17] and Morris.[18] From the Ru-amide, a Ru-η^2-H$_2$ species would be formed upon reaction with hydrogen leading to a hydrido/amine *cis* complex. A Ru-amide species was isolated, starting from a complex of type **B** containing an amino ligand with a methyl-substituted backbone (e.g., H$_2$NCMe$_2$CMe$_2$NH$_2$ vs. H$_2$NCH$_2$CH$_2$NH$_2$), which avoids the dehydrogenation to imino ligands.[18,19] Conversely, Bergens reported that [Ru(H)$_2$(binap)(dpen)] reacts with acetophenone leading to [RuH(OR)(binap)(dpen)] at low temperature.[20] The formation of the Ru-amide and 1-phenylethanol occurs at a subsequent step and an alternative pathway involving a transition state with a partial Ru—O linkage has been proposed.[21] Evidence of the formation of alkoxides [RuH(OR)(PP)(1,2-diamine)] and alcohol complexes [RuH(HOR)(PP)(1,2-diamine)]$^+$, which are involved in the heterolytic cleavage of H$_2$ has been provided by the groups of Morris,[18] Noyori,[22] and Bergens.[23] An alcohol-mediated splitting of H$_2$ in processes promoted by [Cp*Ru(diamine)] catalysts (Cp*=pentamethylcyclopentadienyl) has also been proposed by Ikariya and co-workers[24] and supported through DFT calculations by Brandt and Andersson.[25]

The compounds [RuCl$_2$(PP)(ampy)][26] (**C**) (ampy = 2-aminomethylpyridine) and [(η^6-arene)Ru(O$_3$SCF$_3$)(Tsdpen)][27] (**A**) (Figure 1) are highly active catalysts for both TH and HY reactions, which may occur simultaneously in 2-propanol, depending on the reaction parameters (*T*, solvent, and base).[26d] Unlike the Ru-diamine system **A**, in the asymmetric HY with **C** the alcohol medium dramatically affects both the enantioselectivity (e.g., ethanol vs. *tert*-butanol)[26c] and the rate of the reduction of ketones.[28] Recently, the catalysts **C** have been proven to

promote a series of organic transformations involving the C—H bond activation of alcohols, such as dehydrogenation, allylic alcohol isomerization, ketone α-alkylation,[29] amine alkylation, and amide formation.[30] The literature data confirms that the type of catalysis (TH vs. HY) and the reaction mechanism are subtly controlled by small electronic differences at the metal center, thereby affected by minor modifications of the reaction conditions.[31,32] Therefore, more detailed experiments are still necessary to discriminate the controversial factors that affect the actual nature of the mechanism (inner vs. outer sphere). As an extension of the work on the catalysts of the type **C**, we developed the pincer complexes [MCl(CNN)(PP)] (**D**) (M = Ru,[33] Os;[34] HCNN = 1-(6-arylpyridin-2-yl)methanamine), which are the most efficient catalysts for the TH of carbonyl compounds in 2-propanol, affording high rates (turnover frequency (TOF) $\approx 10^6$ h^{-1}), productivity (turnover number (TON) $\approx 10^5$), and enantioselectivity (enantiomeric excesses (*ee*) up to 99%; Figure 1). These robust systems also display high activity in the asymmetric HY of ketones[33d,35] and in the dehydrogenation (DHY) of alcohols.[36] Recently, Beller and co-workers[37] found that these complexes are highly active catalysts in H$_2$ production from 2-propanol and ethanol, whereas Martín-Matute[38] showed that they catalyze amine alkylation with alcohols. Based on microscopic reversibility, HY catalysts are expected to be efficient also in DHY, namely, the counter-clockwise mechanisms depicted in the lower part of the Schemes 2 and 3. More recently, these Ru and Os pincer complexes of type **D** have also been found to be active in the racemization and deuteration of alcohols.[39] Kinetic and NMR spectroscopic investigations show that in solution, the alkoxide [Ru (CNN)(O*i*Pr)(dppb)] (**1-O*i*Pr**) (dppb = Ph$_2$P(CH$_2$)$_4$PPh$_2$), obtained from the chloride [RuCl(CNN)(dppb)] (**1-Cl**) and NaO*i*Pr, rapidly equilibrates with the hydride [RuH(CNN)(dppb)] (**1-H**) and acetone at RT (Scheme 4).[40]

In this rarely observed example of an oxidation–reduction pathway,[41] both the NH$_2$ function and the protic solvent (2-propanol) play an active role, assisting the activation of the α C—H bond of the isopropoxide through a hydrogen-bonding network.[40] A similar behavior has also been observed for the analogous osmium [Os(CNN)(O*i*Pr)(dppb)],[34] but neither the Ru- nor Os-amide species could ever be detected in solution. Other authors have recently observed the alkoxide–hydride equilibrium reaction for some PNP Ru derivatives.[42] For the pincer complexes **D**, the NH$_2$ function is responsible for the high catalytic activity in both the TH and HY reactions. However, the detection of the alkoxide intermediate instead of amide led us to investigate the energetic profile of the species in-
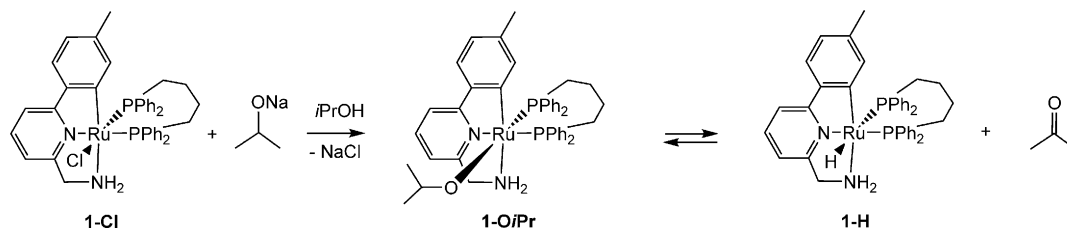
Scheme 4. Fast equilibrium between Ru-O*i*Pr and the Ru-H species.

These are not the final page numbers! ↗↗

volved in the catalytic cycle, in which the NH_2 function and the alcohol media play such a crucial role.

Herein, we report a neutron diffraction study of [Ru(CNN)(OCH_2CF_3)(dppb)] (**1-OCH$_2$CF$_3$**), which is a rare example of a Ru primary amine complex containing an alkoxide ligand). NMR spectroscopic studies were also performed in a solution of the Ru-alkoxide and -hydride species, as well as a DFT computational study on the mechanism of the ketone TH and HY reactions catalyzed by pincer Ru complexes.

Results and Discussion

Synthesis and characterization of a Ru amine-alkoxide pincer complex

The complex **1-OCH$_2$CF$_3$** was easily prepared in 93% yield by treatment of **1-Cl** with NaOCH$_2$CF$_3$, obtained by deprotonation of 2,2,2-trifluoroethanol with NaOEt [Eq. (1)].

1-Cl + NaOCH$_2$CF$_3$ $\xrightarrow{\text{toluene}}$ **1-OCH$_2$CF$_3$** + NaCl (1)
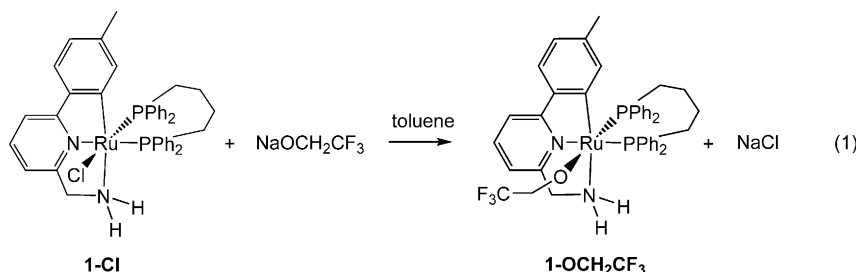
Complex **1-OCH$_2$CF$_3$**, displaying the electron-withdrawing CF$_3$ group, is thermally stable. In fact, no transformation of the amine into an amide donor was observed through displacement of CF$_3$CH$_2$OH, nor does the formation of the Ru-hydride **1-H** occur by elimination of CF$_3$CHO. This species has been fully characterized by NMR spectroscopy. The ^{31}P NMR spectrum of **1-OCH$_2$CF$_3$** in [D$_6$]benzene shows two doublets at $\delta = 57.3$ and 39.6 ppm with a $^2J(P,P) = 35.5$ Hz, which are values very close to those of the analogous alkoxide complexes [Ru-(CNN)(OR)(dppb)] (R=CHMe$_2$,[40a] CHPh$_2$[33b]). In the ^{1}H NMR spectrum, one diastereotopic proton of the CF$_3$CH$_2$O group appears as a quintet at $\delta = 3.87$ ppm with a $^3J(H,F)$ similar to that of the geminal $^2J(H,H)$ (10.5 Hz). The broad signal downfield-shifted to $\delta = 4.36$ ppm is for one NH$_2$ proton, whereas the other is at $\delta = 1.40$ ppm, close to that of the free ligand ($\delta = 1.86$ ppm). Variable-temperature NMR spectroscopic measurements of **1-OCH$_2$CF$_3$** in [D$_8$]toluene show that the two N—H signals at $\delta = 4.34$ and 1.42 ppm (20 °C) do not change significantly from -60 to $+40$ °C, whereas at $+60$ °C they broaden and at $+80$ °C they disappear in the base line. At high temperature, the two protons of the CF$_3$CH$_2$O also undergo a slight modification of their chemical shift, whereas the other protons are not affected. In addition, the ^{31}P NMR spectroscopic measurements show no formation of other species from -60 to $+80$ °C. These data suggest the presence of an intramolecular N—H···O hydrogen-bonding interaction in **1-OCH$_2$CF$_3$** in solution, which is consistent with those reported for the analogous

pincer complexes [RuX(CNN)(dppb)]: One proton of the NH$_2$ group is shifted to low field, depending of the nature of the X substituent (Cl, OPh, OSiMe$_3$, OCOH, or OCOMe; $\delta = 3.41$, 3.50, 4.50, 6.16, 8.40 ppm, respectively), whereas the second proton is upfield ($\delta = 2$–1 ppm range).[33b, 45] In the ^{13}C NMR spectrum, the orthometalated carbon atom appears at $\delta = 186.4$ ppm (dd, $J(C,P) = 15.2$, 8.5 Hz), whereas the carbons of the CH$_2$O and the CNH$_2$ moieties are at $\delta = 65.0$ (q, $J(C,F) = 29.7$ Hz) and 52.1 ppm (d, $J(C,P) = 2.5$ Hz), respectively. Finally, the ^{19}F NMR resonance of the CF$_3$ group is at $\delta = -76.7$ ppm, shifted slightly lowfield with respect to the signal of the corresponding free alcohol ($\delta = -77.8$).

The molecular structure of **1-OCH$_2$CF$_3$** was confirmed by both neutron diffraction and X-ray single-crystal analyses, obtained at 20 and 173 K, respectively. The ORTEP drawing in Figure 2 corresponds to the neutron diffraction structure. As shown in Table 1, the differences between the two structures, obtained with different techniques, are not large, except for the distances involving H atoms, which are known to be underestimated by the X-ray approach. Generally consistent are also the geometric parameters obtained from a DFT optimization (see below), which are also shown in Table 1.

For convenience, the following considerations on geometry refer to the coordinates obtained from the neutron diffrac-
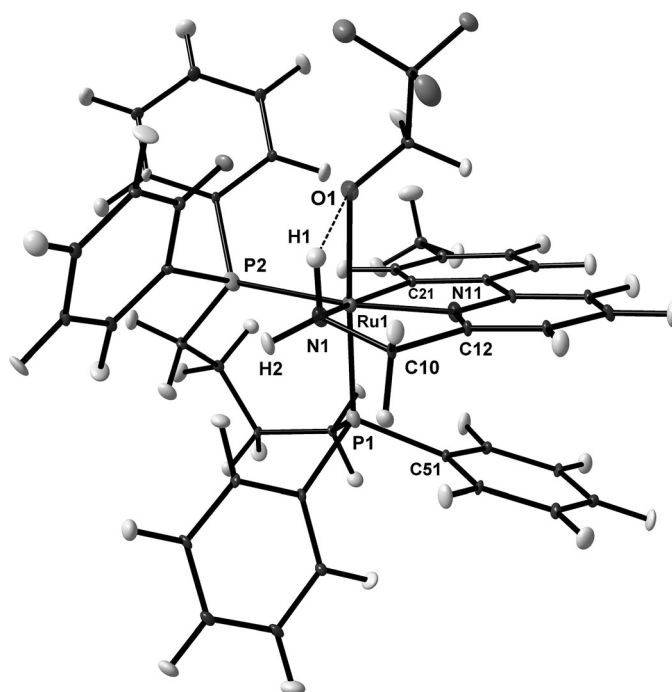

Figure 2. ORTEP-style plot of compound **1-OCH$_2$CF$_3$** (neutron data) in the solid state. Thermal ellipsoids are drawn at the 50% probability level. The dotted line between the atoms H1 and O1 indicates the intramolecular hydrogen bond (2.047(6) Å).

⤴⤴ These are not the final page numbers!

Table 1. Comparison of selected bond length [Å] and angles [°] in the structure of [Ru(CNN)(OCH$_2$CF$_3$)(dppb)] (**1-OCH$_2$CF$_3$**), as derived from neutron and X-ray diffraction studies, as well as calculated by DFT.

	Neutron	X-ray[a]	DFT
Ru1–P1	2.246(4)	2.2428(6)	2.282
Ru1–P2	2.301(4)	2.2910(6)	2.332
Ru1–O1	2.142(3)	2.143(2)	2.143
Ru1–N1	2.232(3)	2.230(2)	2.259
Ru1–N11	2.052(3)	2.054(2)	2.049
Ru1–C21	2.064(3)	2.061(2)	2.043
N1–H1	1.018(6)	0.92	1.030
N1–H2	1.016(6)	0.92	1.014
O1···H1	2.047(6)	2.34	1.895
O1-Ru1-N1	74.8(1)	74.77(7)	73.1
O1-Ru1-N11	84.3(1)	84.40(7)	87.7
O1-Ru1-C21	94.8(1)	94.94(7)	95.2
N1-Ru1-N11	76.9(1)	76.80(7)	76.4
N1-Ru1-C21	155.6(1)	155.35(8)	154.0
N11-Ru1-C21	80.2(1)	79.98(8)	80.1
Ru1-N1-H1	94.5(3)	110	87.9
Ru1-N1-H2	124.4(3)	110	126.4
N1-H1···O1	116.0(4)	100	124.6

[a] Hydrogen atoms H1 and H2 are calculated in ideal positions.

tion data. The ruthenium center has a pseudo-octahedral coordination, with the orthometalated pincer ligand (terdentate) assuming the meridional arrangement. The relatively short Ru–O distance of 2.142(3) Å clearly supports covalency of the metal–alkoxide linkage.[43] The pyridine Ru1–N11 coordination bond, which lies *trans* to one phosphorus donor, is significantly shorter (2.052(3) Å) than the amine Ru1–N1 one (2.232(3) Å). The latter is *trans* to the carbon donor of the arylic ligand, whose *trans* influence is expected to be larger. Possibly, the geometrical constraints of the meridional terdentate pincer ligand may also in part affect the mentioned coordination bonds, because the corresponding bond angles are forced to be acute (80.2(1) and 76.9(1)° for N11–Ru1–C21 and N1–Ru1–N11, respectively). As clearly seen from the Figure 2, the amino N1 atom is biased towards the alkoxide oxygen atom O1 as the O1-Ru-N1 angle is as small as 74.8(1)°. Moreover, one N–H bond is almost coplanar with the Ru1–O1 one (the H1-N1-Ru1-O1 dihedral angle is 6.5(3)°), hence the short H···O distance of 2.047(6) Å.[44] Amongst the consequences of hydrogen bonding, distortion of the tetrahedral geometry of the NH$_2$ moiety is most evident, with an extremely acute Ru1-N1-H1 angle of 94.5(3)° and the corresponding opening of the Ru1-N1-H2 one (124.4(3)°). Previous X-ray data on other known and related carboxylate complexes, such as [Ru(CNN)(OCOR)(dppb)] (R=H, CH$_3$), have already highlighted the important role played by intra- and intermolecular N–H···O hydrogen bonding involving Ru–O and C=O linkages.[45] It is worth noting that alkoxide and phenoxide Ru complexes with a NH function were isolated as alcohol and phenol adducts and that the corresponding X-ray structures showed a six-membered RuO···HO(R)···HN cycle. The corresponding reference compounds are [Ru(CO)$_2${OC-(CF$_3$)$_2$CH$_2$NH$_2$}$_2$]·(CH$_3$OH)$_2$,[46] [RuH(CO)(O*i*Pr)(HN(C$_2$H$_4$P*i*Pr$_2$)$_2$)]·(*i*PrOH),[42] and [RuH(OPh)(H$_2$NCMe$_2$CMe$_2$NH$_2$)(PPh$_3$)$_2$]·PhOH.[47]

In summary, the studies on the alkoxide pincer complexes of general formula [Ru(CNN)(OR)(PP)] suggest that if R is an electron-withdrawing group (i.e., CH$_2$CF$_3$ or CHPh$_2$), the species may be isolated, also owing to the stabilizing intramolecular O···HN hydrogen bonding. From another viewpoint, the stability of the alkoxides in question, compared with that of the Ru hydride **1-H** and the aldehyde or ketone molecules (i.e., the products of the H elimination), can also be ascribed to the high redox potential of the species HCOCF$_3$ or PhCOPh.[4] By contrast, complexes with alkoxide ligands containing an electron-donating group (R=*i*Pr) are more reactive and afford: 1) Adducts with alcohols, leading for example to a RuO···HO(R)···HN six-membered arrangement; 2) formation of Ru-hydride species and carbonyl compounds. The latter reaction is favored by the presence of alcohol and it is probably assisted by a hydrogen-bonding network.[40] The NMR spectroscopic and neutron diffraction studies provide clear-cut evidence of the N–H···O hydrogen bonding in **1-OCH$_2$CF$_3$**, with the four-membered cycle accounting for the exceptional stability of the species. Alkoxide-ruthenium complexes with one NH$_2$ functionality, namely, [(η^6-arene)Ru(OR)(Tsdpen)], and [Ru-H(OR)(diphosphine)(1,2-diamine)], were already suggested to be "catalyst reservoirs" in TH and HY processes involving ketones. In that case, the stabilization of the species was validated by NMR spectroscopic studies in solution and DFT calculations,[14a, 18] whereas in the present work the experimental evidence is provided in a clear and unambiguous manner.

NMR spectroscopic studies on Ru-alkoxide and hydride pincer complexes

The reaction of **1-Cl** with strong bases in alcohol media leads quantitatively to Ru-alkoxide and hydride complexes, which are key species involved in the catalytic TH and HY processes. The pincer system appears simpler to investigate with respect to the well-known *trans*-[RuCl$_2$(PP)(1,2-diamine)] and [(η^6-arene)RuCl((Tsdpen)] Noyori catalysts since: 1) It has only one chloride that can be displaced and 2) the presence of a pincer ligand combined with the bidentate phosphine drastically reduces the degrees of freedom of the complex (e.g., isomerization at the metal center), increasing the stability of the intermediates, which can easily be detected by ^{31}P NMR spectroscopy. This study in solution reveals a complex behavior with several equilibrium reactions and involving the NH function. As described in the Introduction (Scheme 4), compared with **1-OCH$_2$CF$_3$**, the alkoxide [Ru(CNN)(O*i*Pr)(dppb)] (**1-O*i*Pr**), displaying the electron-donating *i*Pr substituent, is not stable at RT and rapidly equilibrates to [RuH(CNN)(dppb)] (**1-H**) and acetone in [D$_6$]benzene. Addition of 2-propanol to **1-O*i*Pr** gives the alcohol adduct [Ru(CNN)(O*i*Pr)(dppb)]·(*i*PrOH)$_n$, which converts into the hydride **1-H** with an apparent global rate of (5.4±0.2) s^{-1} at 25°C. The added alcohol has been proven to increase the rate of the alkoxide–hydride exchange.[40a]

We now focus on the usage of OEt$^-$/EtOH in place of O*i*Pr$^-$/*i*PrOH since the catalytic activity of the pincer-Ru complexes depends on the alcohol media: Whereas ethanol is the solvent of choice in HY (see below), 2-propanol is employed in TH.

These are not the final page numbers! ↗↗
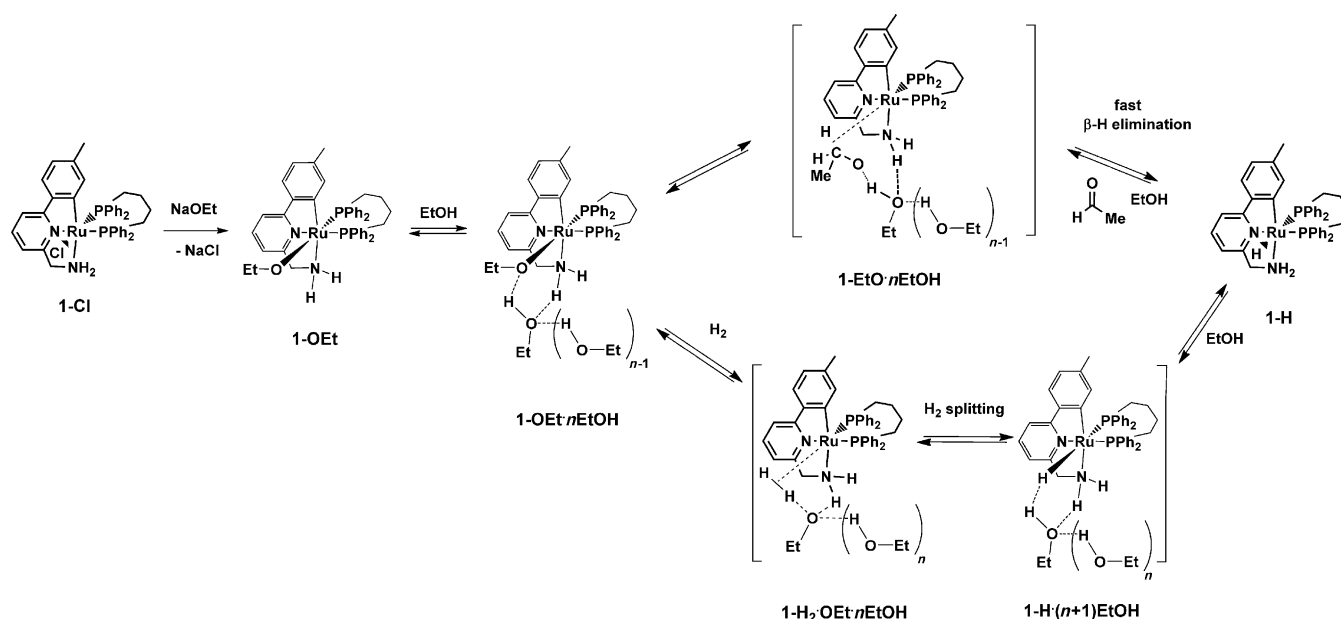
Scheme 5. Formation of the hydride **1-H** from the alcohol-adduct ethoxide **1-OEt·n EtOH** through reversible hydrogen elimination and heterolytic dihydrogen splitting.

Treatment of the chloride precursor **1-Cl** with NaOEt in [D$_6$]benzene leads to the ethoxide [Ru(CNN)(OEt)(dppb)] (**1-OEt**), which in the presence of EtOH affords the alcohol adduct [Ru(CNN)(OEt)(dppb)]·(EtOH)$_n$ (**1-OEt·n EtOH**). This species equilibrates with the hydride **1-H** and acetaldehyde,[48] as inferred from NMR spectroscopic measurements, through a fast and reversible H-elimination reaction. In turn, the hydride complex **1-H** is slowly protonated by the alcohol media leading to **1-OEt·-n EtOH** and producing H$_2$, in a reversible fashion. Scheme 5 indicates that the pincer alkoxide **1-OEt·n EtOH** is alternatively able to activate the ethoxide C—H bond or the H$_2$ molecule; the two processes being the key for understanding the catalytic TH, HY, and DHY reactions.

In the presence of EtOH (3 equiv) the ^{31}P NMR spectra indicate that **1-OEt** and **1-OEt·n EtOH** (1:3 molar ratio, respectively) equilibrate with the hydride **1-H** (**1-H/1-OEt·n EtOH** = 3:4) at 25 °C (see Supporting Information, Figure S4). When a greater amount of alcohol (10 equiv) is used, compound **1-OEt·n EtOH** is obtained through solvation of **1-OEt** and protonation of **1-H** with concomitant formation of H$_2$ (**1-H/1-OEt·n EtOH** = 1:7; see Supporting Information, Figure S5). By using 25 equiv of EtOH, compounds **1-OEt** and **1-H** are converted almost quantitatively to **1-OEt·n EtOH** (>95%). The ^{31}P NMR spectra of **1-OEt** and **1-OEt·n EtOH** in [D$_6$]benzene with EtOH (10 equiv) show two doublets at

$\delta = 54.8$ and 40.2 ppm with $^2J(P,P) = 33.0$ Hz, and at $\delta = 54.7$ and 44.5 ppm with $^2J(P,P) = 34.5$ Hz, respectively, values similar to those of **1-OCH$_2$CF$_3$** and **1-OiPr**.[40a] The ^{31}P NMR signals for the hydride **1-H** are at $\delta = 65.7$ and 34.6 ppm with a significantly lower $^2J(P,P) = 17.2$ Hz. Importantly, the hydride **1-H** and the alkoxide complexes **1-OEt** and **1-OEt·n EtOH** are all in exchange at 25 °C, as observed through a ^{31}P-^{31}P NOESY experiment (see Supporting Information, Figure S6). ^{1}H-^{1}H COSY, TOCSY, and NOESY correlation experiments carried out at different Ru/EtOH molar ratios, allow the assignment of the proton chemical shifts of the **1-OEt·n EtOH** and **1-H** complexes (Figure 3 and see Supporting Information, Figures S7 and S8).

The ^{1}H NMR spectrum of **1-OEt·n EtOH** in [D$_6$]benzene with EtOH (25 equiv) shows the two NH protons at $\delta = 3.60$ and 1.85 ppm in mutual exchange and with the EtO—H proton at
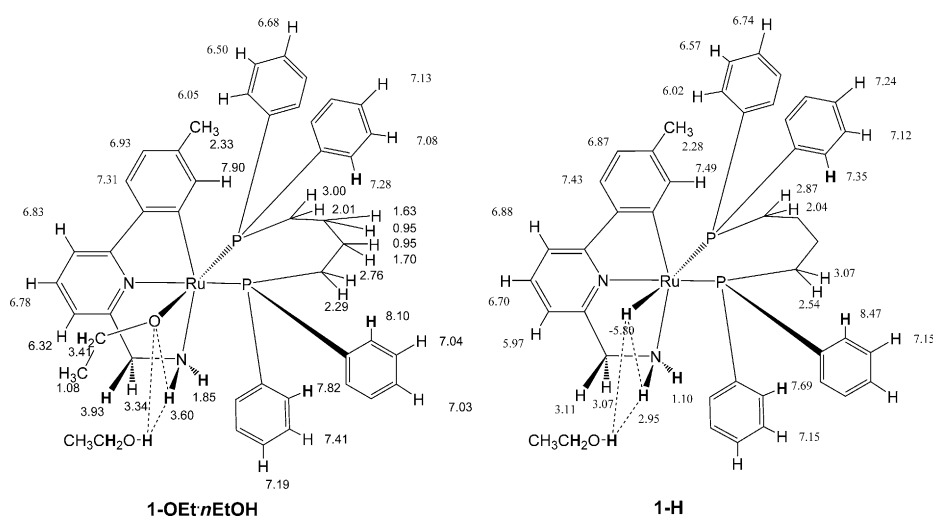

Figure 3. ^{1}H NMR spectroscopic assignments for the ruthenium ethoxide **1-OEt·n EtOH** and the hydride **1-H** complexes. Protons involved in exchange processes or showing NOE contacts are in bold (**H**).

↖↖ **These are not the final page numbers!**

$\delta = 2.19$ ppm. The downfield signal ($\delta = 3.60$ ppm) originates from the synperiplanar NH proton with respect to the Ru–O bond, consistent with the presence of an O···H–N hydrogen bond, and shows nuclear Overhauser effect (NOE) contacts with the *ortho*-phenyl protons at $\delta = 7.82$ ppm (see Supporting Information, Figures S7 and S8). The other NH proton ($\delta = 1.85$ ppm) also shows NOE contacts with the *ortho* protons ($\delta = 7.28$ ppm) of the phenyl substituent bound to the phosphorus atom, which lies *trans* to the Ru–O bond. Notably, the NCH proton at $\delta = 3.93$ ppm and the *ortho* protons ($\delta = 8.10$ and 7.82 ppm) of the two phenyl rings on the side of the alkoxide show contacts with the EtO–H proton, suggesting that EtOH is involved in a hydrogen-bonding network with the Ru–NH$_2$/–OEt moiety. Moreover, the quartet at $\delta = 3.41$ ppm is for the OCH$_2$ signal of the OEt$^-$ ligand and EtOH that rapidly exchanges, possibly through a RuO(Et)···H–OEt hydrogen bond, in agreement with the studies on [Ru(CNN)(OCHPh$_2$)-(dppb)]···H–OCHPh$_2$ (70 ms at 20 °C).[33b]

As for **1-OEt·n EtOH**, the NH$_2$ protons of the hydride **1-H** ($\delta = 2.95$ and 1.10 ppm) show mutual exchange and with the EtO–H proton at $\delta = 2.19$ ppm, as inferred from ^{1}H-^{1}H NOESY experiments (see Supporting Information, Figure S9). The Ru–H hydride ($\delta = -5.80$ ppm) shows NOE interactions with the NH$_2$ protons and with the *ortho* protons ($\delta = 8.47$ and 7.69 ppm) of the two phenyl rings bound to the P *trans* to the pyridine nitrogen. The resonance at $\delta = 2.95$ ppm has been assigned to the synperiplanar NH proton with respect to the Ru–H bond on the basis of the NOE contact with the hydride proton, whereas the signal at $\delta = 1.10$ ppm is assigned to the NH proton showing NOE interaction with the *ortho* protons ($\delta = 7.35$ ppm) of the phenyl ring at the P atom *trans* to the hydride. Therefore, both in the hydride **1-H** and in the alkoxide **1-OEt·n EtOH**, the synperiplanar NH proton to the Ru–H and Ru–OR bonds, respectively, is shifted downfield, suggesting an involvement in a hydrogen-bonding interaction. The result for **1-H** should be compared with those reported by Noyori[22] and Bergens[20b] for the system [RuH(X)(diphosphine)(diamine)] in which the synperiplanar NH to the Ru–H is shifted upfield. For **1-H**, an intramolecular Ru–H···H–N interaction has also been proposed on the basis of the Ru–H stretching that is remarkably lower in comparison to the corresponding N-methylated hydride complex (1743 vs. 1811 cm^{-1}, respectively).[33b] Interestingly, the Ru–H resonance at $\delta = -5.80$ ppm rapidly exchanges both with the EtO–H proton and the OCH$_2$ protons ($\delta = 3.41$ ppm) of **1-OEt·n EtOH**, (Scheme 5). With a small amount of alcohol (3 equiv) the H–Ru of **1-H** shows a NOE contact with the H–OEt, whereas with 15 equiv of EtOH a RuH/EtOH exchange is observed. This behavior suggests the formation of an H$^+$···H$^-$ interaction of the alcohol OH group with the hydride (Scheme 5), leading to **1-OEt·n EtOH** through H$_2$ elimination. The progressive addition of EtOH at 25 °C caused a reduction of **1-H** with H$_2$ formation ($\delta = 4.50$ ppm in [D$_6$]benzene) and a significant upfield shift of the ^{1}H NMR hydride signal ($\delta = -5.58$, -5.69, and -5.93 ppm at EtOH/**1-H** = 0, 15, 25), whereas the ^2J(P,P) increases from 17.2 to 18.3 Hz, suggesting the fast formation of a dihydrogen bonding adduct Ru–H···HOEt[49] of the type **1-H·(n + 1) EtOH** (Scheme 5). When the

solution of **1-OEt·n EtOH** containing 25 equiv of EtOH is kept under H$_2$ (5 atm), the hydride **1-H**, which is present in trace, starts to form through hydrogen splitting, affording a mixture **1-H/1-OEt·n EtOH** = 2:3 (see Supporting Information, Figure S10). The ^{1}H NMR spectra also revealed the formation of a new species at $\delta = -7.17$ ppm in a molar ratio of about 2:1 with respect to **1-H**, which was attributed to **1-H$_2$·OEt·n EtOH** (Scheme 5, Figure 4).
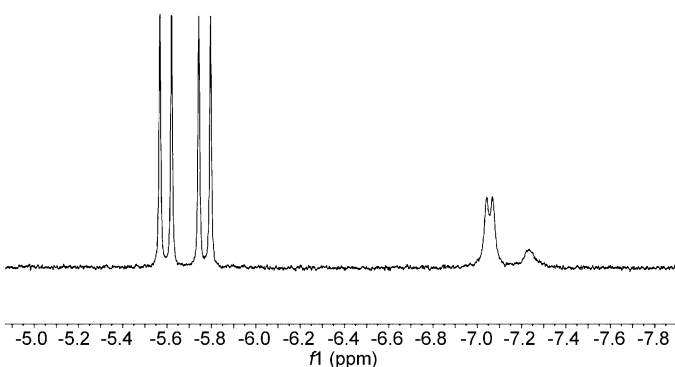

Figure 4. ^{1}H NMR spectrum of **1-H** in the hydride region in presence of ethanol and H$_2$.

Interestingly, NOESY experiments show that the hydrogen at $\delta = -7.17$ ppm exchanges not only with the OCH$_2$ group of **1-OEt·n EtOH**, as for **1-H**, but also with H$_2$ present in solution (see Supporting Information, Figure S9). Apparently, no fast exchange of the nucleus at $\delta = -7.17$ ppm with the H–OEt proton and with the Ru-hydride **1-H** occurs (Scheme 5). Strikingly, the scalar coupling pattern of the hydride-like signal at $\delta = -7.17$ ppm to the *trans* phosphorus exhibits the typical distortion expected from cross-correlation of chemical shift anisotropy and dipole–dipole interaction (CSA-DD), with a line shape that appears substantially broadened with respect to the corresponding Ru-hydride **1-H** resonance.[50]

These studies show that the presence of the NH$_2$ function in the pincer complexes stabilizes both the alkoxide and hydride complexes through intramolecular hydrogen bond interactions involving the N–H parallel to the OR and H ligands, and also through hydrogen bonds with the external alcohol, which weaken and render more reactive the Ru–O and Ru–H bonds. Whereas the Ru-alkoxide complex acquires more stability, the latter linkage becomes more labile. The catalytically active hydride **1-H** is formed from the Ru-alkoxide through two pathways, namely, through a fast hydrogen elimination and by a slower dihydrogen splitting (Scheme 5), indicating that the reduction of carbonyl compounds with H$_2$ in alcohol media occurs through two parallel routes. The studies on the HY of ketones with the [(η^5-C$_5$(CH$_3$)$_5$)RuCl(cod)] (cod = 1,5-cyclooctadiene)/1,2 diamine system, reported by Ikariya, revealed that H$_2$ exchanges rapidly with the HO alcohol proton and suggest that the alcohol participates in the H$_2$ activation by the Ru-amide to generate the Ru–H species.[24] An implication of the latter is that the Ru-amine-alkoxide complex with its strong O···H–N hydrogen bonding can be in equilibrium with the Ru-

Ru-amine-alkoxide   *Ru-amide-alcohol*   *Ru-amide*   + EtOH
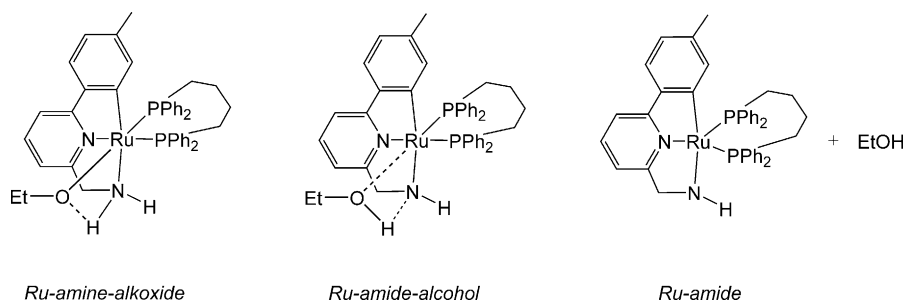
Figure 5. Ru-amine-alkoxide versus Ru-amide-alcohol.

amide-alcohol adduct or with a five coordinated Ru-amide species with the formed alcohol (Figure 5).

Although in our studies we have not seen any amido intermediate for the pincer ruthenium complexes, in the route to the hydride **1-H** complex it cannot be excluded that such a Ru-amide-alcohol species may be rapidly formed and transformed. The DFT calculations reported below do in fact support such a possibility.

Catalytic HY of ketones catalyzed by 1-Cl

The pincer complexes [MCl(CNN)(PP)] (M = Ru and Os; PP = Josiphos) display a high catalytic activity in both asymmetric TH and HY of ketones, leading to alcohols with up to 99 % *ee* at low catalyst loading and achieving extremely high rates.[33d,34,35] Complex **1-Cl** bearing PP = dppb was proven to catalyze the reduction of ketones and aldehydes through TH in 2-propanol heated at reflux using 0.01–0.001 mol % of Ru, with TOF up to 10^6 h^{-1}.[33] The derivative **1-Cl** efficiently promotes the HY of acetophenone (0.5 M) at 40 °C with H$_2$ (5 atm) in the presence of KOtBu (2 mol %). The effect of the alcohol media (ROH; R = Me, Et, iPr) has been investigated and it was shown that EtOH affords the best performance with complete conversion of MeCOPh in 30 min, using 0.01 mol % of **1-Cl** (see Supporting Information, Figure S11). The TOF[51] values are 3.1×10^4, 6.5×10^4, and 2.9×10^4 h^{-1} in MeOH, EtOH, and iPrOH, respectively. It is worth noting that although in MeOH and iPrOH the rates are much the same, in MeOH the reaction occurs through HY and not through TH on account of the high redox potential of formaldehyde.[4] In fact, in MeOH and in the absence of H$_2$, less than 5 % of 1-phenylethanol was observed, whereas in iPrOH, 90 % of conversion was achieved as a result of the TH equilibrium reaction.

We also investigated the influence of the base concentration on the catalytic activity of **1-Cl** in the HY in ethanol. Without a base, complex **1-Cl** is practically inactive; the highest rate was observed with KOtBu in the range of 1–3 mol % (Figure 6). A higher base concentration has a detrimental effect; the complex **1-Cl** is almost inactive with more than 6 mol % of KOtBu. These results have to be compared with those obtained in 2-propanol in TH, in which an increase of the base resulted in a more pronounced catalytic activity of **1-Cl**.[40b] The chiral derivative [RuCl(CNN-Me)((S,R)-Josiphos-OMe, 3,5-Me$_2$)] (**1'-Cl**),[33d] containing a more basic phosphine, gives (S)-1-phenylethanol

(92 % *ee*) with lower TOF numbers with respect to **1-Cl**; the best performance was achieved with a higher base concentration (6 mol %; Figure 6).

In contrast to TH, these results show that the catalytic HY occurs in a certain range of base concentration, which is related to the basicity of the phosphine. This behavior can be ascribed to the necessity of the displacement of the alkox-
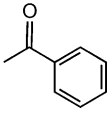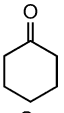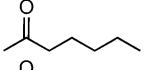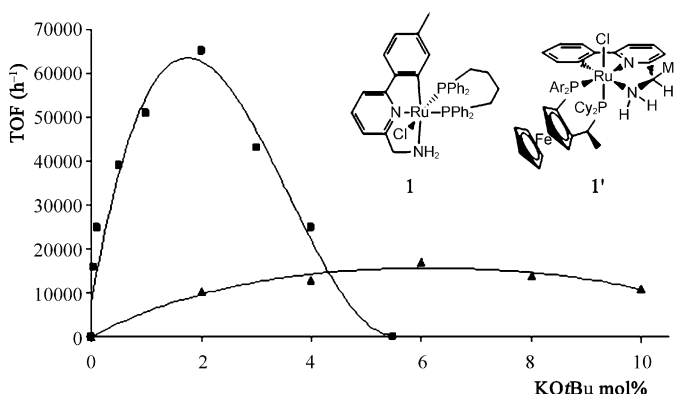

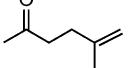**Figure 6.** Catalytic HY of acetophenone (0.5 M) with H$_2$ (5 atm) at 40 °C using 0.01 mol % of **1-Cl** (■) and [RuCl(CNN-Me)((S,R)-Josiphos*)] (**1'-Cl**)[33d] (▲) (Ar = 4-OMe-3,5-Me$_2$C$_6$H$_2$) at different KOtBu concentration in ethanol.

ide ligand for the coordination of the H$_2$ to achieve the dihydrogen splitting (Scheme 5 and the DFT study). We also investigated the dependence of the rate of HY on the temperature. With **1-Cl** (0.01 mol %) and in presence of 2 mol % of base, acetophenone is quantitatively reduced under 5 atm of H$_2$ in EtOH in 1 h at 20° and 10 min at 90 °C with a rate which increases regularly with the temperature (TOF = $1.5–9.3 \times 10^4$ h^{-1}; see Supporting Information, Table S1). The relatively low increase of the rate, with respect to the Arrhenius relationship, is likely due to the hydrogen availability in solution, which depends on the temperature and the diffusion process. Employing optimized reaction conditions, complex **1-Cl** efficiently catalyzes the HY of alkyl-aryl and dialkyl ketones. As shown in Table 2, the substrates cyclohexanone, 2-heptanone, and 5-methyl-2-hexenone (0.5 M) are reduced by using 0.01 mol % of **1-Cl** under 5 atm of H$_2$, affording quantitative conversion within 1 h at 40 °C. With 5-methyl-2-hexanone, selective HY of the carbonyl group was observed with no isomerization or hydrogenation of the terminal C–C double bond.

DFT study of the reaction mechanism of transfer hydrogenation (TH) and hydrogenation (HY)

Calculations were performed by using a DFT/PBE0 approach (see the Computational Details). The TH and HY reactions in-

↖↖ These are not the final page numbers!

Table 2. Catalytic HY of ketones (0.5 M) with **1-Cl** (0.01 mol%) in EtOH under 5 atm H_2 at 40 °C in the presence of KOtBu (2 mol%).

Ketone	Conv. [%][a]	t [min]	TOF [h^{-1}][b]
(acetophenone)	>99	15	6.5×10^4
(cyclohexanone)	>99	60	1.7×10^4
(heptan-2-one)	99	60	2.4×10^4
(unsaturated ketone)	94	60	1.0×10^4

[a] The conversion was determined by GC analysis. [b] Turnover frequency (moles of ketone converted to alcohol per mole of catalyst per hour) at 50% conversion.

volving the alkoxide **1-OR** and hydride **1-H** species, based on the fragment [Ru(CNN)(dppb)]$^+$ (**1**), were analyzed. These complexes were modeled replacing the phenyl groups of the diphosphine ligand by methyl substituents and the methyl at the CNN pincer ligand by an H atom, namely [Ru(CNN′)-(dmpb)]$^+$ (**2**) (HCNN′ = 2-aminomethyl-6-(phenyl)pyridine; dmpb = Me$_2$P(CH$_2$)$_4$PMe$_2$). One explicit molecule of 2-propanol was included in the model. Several authors have shown that the outcome of calculations is strongly influenced by the alcohol solvent molecule.[52,53] Our calculations provide evidence that during the chemical transformations, the cationic metal fragment **2** can undergo deprotonation of the amino ligand, affording the uncharged amide complex, which is indicated as **2′**. All the other species in the processes are defined according to the previous nomenclature, adding the anionic ligand and/or other molecules interacting with the complex. The compound **2-H·iPrOH·Me$_2$CO** represents the model hydride complex **2-H** with one alcohol molecule **iPrOH** (solvation) and one approaching ketone substrate **Me$_2$CO**.

Transfer hydrogenation (TH)

The alkoxide complex [Ru(CNN)-(OCH$_2$CF$_3$)(dppb)] (**1-OCH$_2$CF$_3$**) was fully optimized and the calculated structural parameters (reported in Table 1) are in good agreement with the neutron and X-ray diffraction structures. The largest difference concerns the intermolecular O1···H1 hydrogen bonding in the O1···H1–N1 arrangement (Figure 2), which is about 0.15 Å shorter than in the neutron

structure and up to three times shorter than in the X-ray structure. Thus, the H···O distance of only 1.895 Å appears overestimated by the calculations and the trend also corresponds to the largest deformation from the ideal tetrahedral value for the angle Ru1-N1-H1 angle (87.9° vs. the 94.5(3)° value of the neutron structure).

To clarify the mechanism of the reduction of ketones to alcohols through TH, we have analyzed the single steps for a reaction, starting from the model Ru-hydride **2-H** and acetone in 2-propanol, leading to the corresponding Ru isopropoxide product. The energy profile is outlined in Figure 7 and the associated geometric features of all the optimized species are shown in Figure S12 (see Supporting Information).

The energies (in kcal mol^{-1}) were obtained with the polarizable continuum model (PCM) model using isopropanol as a solvent (implicit and explicit solvent; see Computational Details). The process starts with the adduct **2-H·iPrOH·Me$_2$CO**, which undergoes an internal nucleophilic attack of the metal hydride to the acetone carbon atom, leading to **2-iPrO·iPrOH**, through the transition state **TS$_1$**. In **2-iPrO·iPrOH**, the formed C–H bond is relatively long (1.235 Å), with a residual Ru–H interaction indicated by the short 1.860 Å distance. In turn, the formed isopropoxide group interacts with the 2-propanol proton, leading to **2-iPrOH·OiPr**, in which the Ru···H bond is very weak, the C–H and Ru–H distances being 1.159 and 1.998 Å, respectively. At this point, the newly formed isopropoxide group can abstract one H atom of the coordinated amine, since the corresponding O···H and N···H separations are much the same (1.474 and 1.481 Å, respectively). In the following step, the amide species **2′-iPrOH·iPrOH**, solvated by two hydrogen-bonded 2-propanol molecules (the O–H and N···H distances are 0.998 and 1.758 Å, respectively), is formed through the transition state **TS$_3$**. This species corresponds to a five-coordinated ruthenium(II) complex, the metal unsaturation being partially compensated by a Ru=N$_{amido}$ π-bond as short as 2.085 Å, whereas the corresponding Ru–N$_{amino}$ distance in **2-H·iPrOH·Me$_2$CO** is much longer (2.266 Å). The **2′-iPrOH·iPrOH** without one alcohol molecule, which can be designated as **2′-iPrOH**, has a shorter Ru=N$_{amido}$ bond (2.026 Å, Wiberg index (WI=0.474), reflecting how the solvating molecule tunes the strength of this bond. In view of the almost planar geometry of the amido group, its p$_\pi$ lone pair is dative towards the apically oriented Ru p orbital. The latter interaction stabilizes the
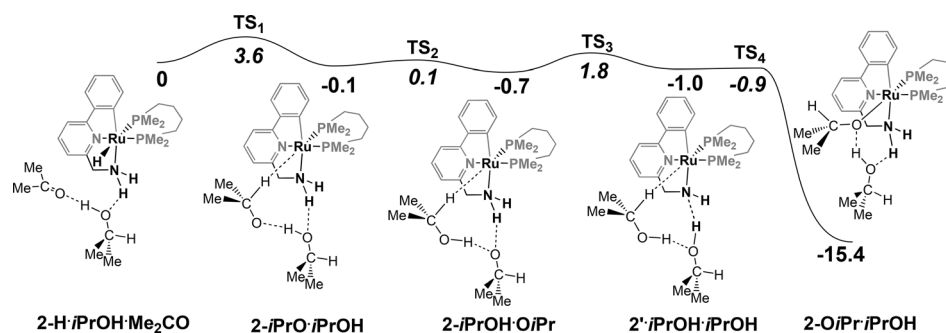
Figure 7. Energy profile of the reaction between the Ru-H complex and acetone leading to the Ru-isopropoxide assisted by one 2-propanol molecule (solvent-corrected E values [kcal mol^{-1}]).

five-coordinated ruthenium(II) amido species, whereas the cationic amine species **2** could never be optimized. The lower coordination number in **2′-iPrOH·iPrOH** is counterbalanced by this amide-ligand π-donation. The final step towards the isopropoxide species **2-OiPr·iPrOH** is the most exergonic one (-15.4 kcal mol^{-1}), after bypassing a negligible energy barrier at **TS₄**. Since all the barriers **TS₁–TS₄** are small (< 3.6 kcal mol^{-1}), the transformation of the hydride into the isopropoxide derivative is a facile process. This last step corresponds to a concerted double proton transfer in **2′-iPrOH·iPrOH**. One 2-propanol transfers one proton to the amide, reforming the amino ligand, and receives another proton from the second 2-propanol, which converts into the isopropoxide ligand.

The optimized structure of **2-OiPr·iPrOH** compares well to that of **1-OCH₂CF₃**. The presence of the electron-withdrawing CH₂CF₃ substituent in the alkoxide leads to a short Ru—O distance (2.143 Å) compared with the model complex (2.199 Å), suggesting that electron-withdrawing substituents stabilize the Ru alkoxide versus the Ru-hydride species, shifting the equilibrium towards the right side of the profile in Figure 7. Based on this profile, a catalytic cycle can be envisaged in which the ketone substrate is reduced to alcohol, affording the amide **2′-alcohol·iPrOH**. Replacement of alcohol by 2-propanol leads back to the hydride **2-H·iPrOH·Me₂CO**, which undergoes displacement of acetone with the incoming ketone and closing the cycle (Figures 7 and 9, below).

The energy differences between the four intermediates connected by **TS₁₋₄** are very small. The largest energy barrier of 3.6 kcal mol^{-1} is associated with hydrogen transfer from Ru to the ketone (**TS₁**), affording rapid exchange among the species. The alkoxide complex **2-OiPr·iPrOH** is clearly the most stable species along the profile. The value of ΔE calculated between the hydride **2-H·iPrOH·Me₂CO** complex and the alkoxide **2-OiPr·iPrOH** (-15.4 kcal mol^{-1}) is close to the ΔH value of -11.4 kcal mol^{-1}, which was obtained by ^{31}P NMR spectroscopic measurements for the equilibrium between the system **1-H/acetone** and **1-OiPr·nHOiPr** in 2-propanol/[D₆]benzene.[40a] The corresponding ΔG for **2-H·iPrOH·Me₂CO/2-OiPr·iPrOH** is -9.1 kcal mol^{-1} at 298 K, indicating a negative entropic contribution, consistent with a more-ordered alkoxide-versus-hydride system. All these energies are overestimated owing to the limitations of the model used. Nevertheless, the calculated barrier of 14.5 kcal mol^{-1} (**TS₄**) is not very high and can be overcome, allowing the formation of hydride, a process that is favored by increasing the temperature. In the presence of ketone substrates containing electron-withdrawing groups, the catalysis is slower because of the larger stability of the resulting alkoxide complex. Since the catalysis is carried out in 2-propanol, the displacement of the alkoxide finally occurs because of the high concentration of 2-propanol. The reaction profile calculated for benzophenone Ph₂CO as a substrate in the presence of 2-propanol is similar to that with acetone in Figure 7, with a barrier for the first step of 6.8 kcal mol^{-1}, whereas the alkoxide **2-OCH-Ph₂·iPrOH** is stabilized by -15.9 kcal mol^{-1} (see Supporting Information, Figure S13). The very small activation barriers calculated for **TS₁–TS₄** imply small geometric variations with respect to the relevant intermediates. Only the first transition state

(**TS₁**) differs significantly from **2-H·iPrOH·Me₂CO**, since the transferring hydride is as close as 1.636 Å to the acetone carbon atom, whereas the interaction is totally absent in **2-H·iPrOH·Me₂CO**. Also at **TS₁**, the Ru—H bond has stretched from 1.649 to 1.717 Å (see Supporting Information, Figure S12). This is most likely associated with the strong *trans* effect exerted by the opposite P atom, whose donor capability seems crucial for the lability of the hydride, hence the high catalytic activity of the system. Also, the Ru—P bond in question is significantly strengthened (from 2.347 to 2.266 Å) in going from **2-H·iPrOH·Me₂CO** to **2-iPrO·iPrOH** when the Ru-H elongates as mentioned. Interestingly, the same Ru—P length is very short (2.203 Å) in the five-coordinate amide complex **2′-iPrOH·iPrOH**, stabilized by the Ru=N$_{amido}$ bond. No evidence of the amido species of the type **2′-iPrOH·iPrOH** has been provided experimentally due to the fast equilibrium being shifted towards the more stable alkoxide product **2-OiPr·iPrOH**. However, the intermediate **2′-iPrOH·iPrOH**, which plays a relevant role in the transfer hydrogenation mechanism, should not be too stable because it would result in poor catalytic performance.

Note that the present calculations have been performed using an assisting alcohol molecule, contrary to the reaction mechanism reported by Noyori.[14a] In the present system, the alcohol molecule plays an essential role in facilitating the formation of an amide complex leading to the solvated adduct species **2′-iPrOH·iPrOH**. The role of the solvent and the need for a realistic model have been demonstrated in the TH of formaldehyde catalyzed by Ru complexes of **A** type (see the Introduction), by using DFT and Carr–Parrinello molecular dynamics simulation in methanol.[52] In more recent work, Dub and Ikariya examined in detail the effect of inclusion of specific and nonspecific solvation in TH with **A**-type catalysts and showed that the calculated barriers decrease significantly when explicit solvent is present, and that the nature of the process is not so clear-cut.[52] Also, the proton source for the second protonation of the ketone, from RO$^-$ to ROH, does not have to be the amine but can be the alcohol. Our profile described in Figure 7 also shows that the same protonation (second step, over **TS₂**) is carried out by the alcohol, which in turn will receive another proton from the coordinated NH₂. The solvent acts as a hydrogen shuttle and this model, which can be considered more realistic, shows the subtleties of hydrogen bond-assisted proton transfer reactions.

Interestingly, the reaction between the chiral pincer complex [RuCl(CNN){(S,S)-Skewphos}] (Skewphos = Ph₂PCH(Me)-CH₂CH(Me)PPh₂) and the prochiral ketone CF₃CO(4-C₆H₄F) gave [Ru(CNN){OCH(CF₃)(4-C₆H₄F)}{(S,S)-Skewphos}] as a mixture of two isomer alkoxides in 67% diastereomeric excess. This value is much the same as that of the enantiomeric excess of the alcohol CF₃CHOH(4-C₆H₄F) (64% *ee* of the *R* enantiomer) obtained in the asymmetric catalytic TH using [RuCl(CNN){(S,S)-Skewphos}].[40a] These results are consistent with the profile of Figure 7, suggesting that the chiral recognition of the prochiral ketone occurs in the initial step for both the stoichiometric and catalytic reactions.

↖↖ **These are not the final page numbers!**

Hydrogenation (HY)

As shown in the lower part of Scheme 5, the Ru-hydride complex **1-H** can also be generated by reaction of the alkoxide species **1-OEt·OEtH** with dihydrogen, thus allowing the catalytic reduction of ketones with H_2 in place of 2-propanol (HY vs. TH).

The computed energy profile in Figure 8 starts from the optimized amide species **2′-iPrOH·H_2**, which results from the amide adduct **2′-iPrOH·iPrOH** of Figure 8 after substitution of one alcohol molecule with dihydrogen.
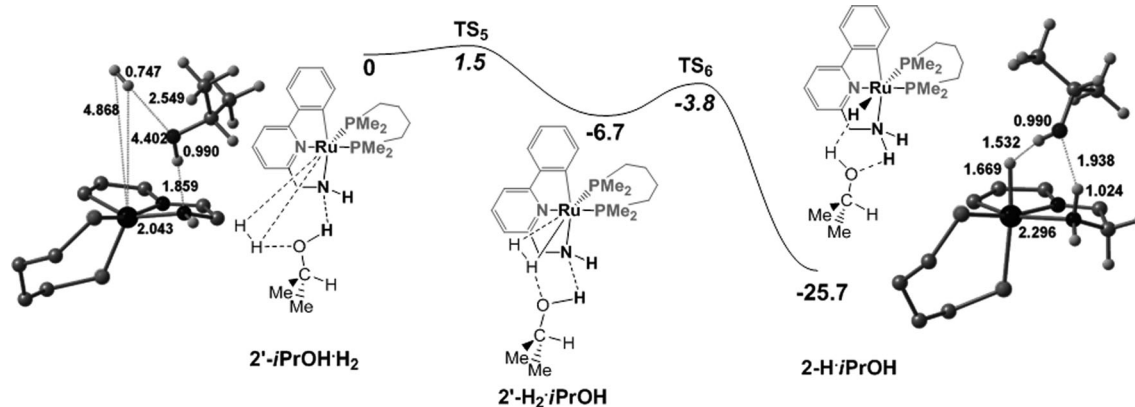
the small **TS$_6$** barrier in the last step. Regardless of the underlined extra stabilization, the product **2-H·iPrOH** corresponds to the starting hydride complex of Figure 7 that interacts with the ketone substrate (**2-H·iPrOH·Me$_2$CO**). These results confirm that the hydride complex **2-H·iPrOH**, which is the key species for the catalytic reduction of ketones, can be generated easily either from 2-propanol through reversible H-elimination or from H_2 splitting, because of the low activation barriers for both reactions in the presence of alcohol molecules. In addition, according to this mechanism, the rate of the hydrogenation depends on the base concentration since a small amount

Figure 8. Pathway for the formation of the ruthenium-hydride complex **2-H·iPrOH** from dihydrogen (solvent corrected E values, kcal mol^{-1}).

The approaching H_2 molecule is almost perpendicularly directed towards the unsaturated metal (Ru–H distances of 4.868 and 4.402 Å, see Supporting Information, Figure S14) and is laterally attracted by the oxygen atom of the alcohol molecule (2.549 Å). Then, after passing a very small barrier of 1.5 kcal mol^{-1} at **TS$_5$**, it converts into **2′-H_2·iPrOH**, in which H_2 is dihapto-coordinated to the metal with Ru–H distances of 1.810 and 1.873 Å. The slight asymmetry is also due to the interaction of one H atom with the adjacent iPrOH oxygen atom (2.197 Å). The H–H bond is only slightly elongated from 0.747 to 0.810 Å. At the following **TS$_6$** (2.9 kcal mol^{-1}), the H–H bond is almost unchanged (0.837 Å), but one H atom is significantly closer to the oxygen (1.746 Å) and further from the metal (≈ 2 Å). Simultaneously, the terminal H atom of the alcohol lies almost half way between the O and N atoms (separation of 1.293 and 1.200 Å, respectively). Eventually, the amido complex converts into the amino one **2-H·iPrOH**, in which only one hydride H atom is bound to the metal (1.669 Å). However, such a Ru–H bond is involved in a six-membered hydrogen-bonding ring with the H–O and H–N bonds of the adjacent alcohol and amine moieties, respectively. Thus, the separations O···H–N and Ru–H···H–O are as short as 1.938 and 1.532 Å, with the latter value indicating some residual interaction between the H atoms of the original H_2 molecule. Such M–H···H–X (X = N, O, S) arrangements have been previously ascertained in solid state structures and spectroscopic experimental data,[54] as well as calculated structures.[55] The features of **2-H·iPrOH** justify the large stabilization energy of −19.0 kcal mol^{-1} after passing

of base (alkoxide) is necessary to generate the catalytically active Ru-hydride. By contrast, a strong excess of base results in the accumulation of the alkoxide complex slowing down the catalysis, in agreement with the experimental kinetic results of Figure 6 and leading to an optimal "pH window" for the catalytic hydrogenation.

We should also emphasize the role of the 2-propanol molecule in the HY reaction, assisting H-H splitting in **2′-H_2·iPrOH**, through the O−H···H−H hydrogen bond (Figure 8 and see Supporting Information, S14). It also stabilizes the hydride complex **2-H·iPrOH** in a way that allows the easy approach of the incoming ketone substrate. This type of interaction between an alcohol (or water) molecule and coordinated dihydrogen has been proposed before in other hydrogenation reactions, in which the reaction mechanism was computationally studied in a model containing explicit and implicit solvent.[31,56]

The catalytic cycle

The energy relationships between the main intermediates involved in both TH and HY reactions are summarized in Figure 9. The values refer to the model ruthenium-hydride **2-H** and the substrates Me$_2$C=O and Ph$_2$C=O, in the presence of 2-propanol, namely, **2-H·iPrOH·R$_2$CO** (R = Me, Ph). In both catalytic reactions the reduction of the substrate ketone occurs in **2-H·iPrOH·R$_2$CO**, leading to the amide alcohol adduct **2′-iPrOH·R$_2$CHOH**.

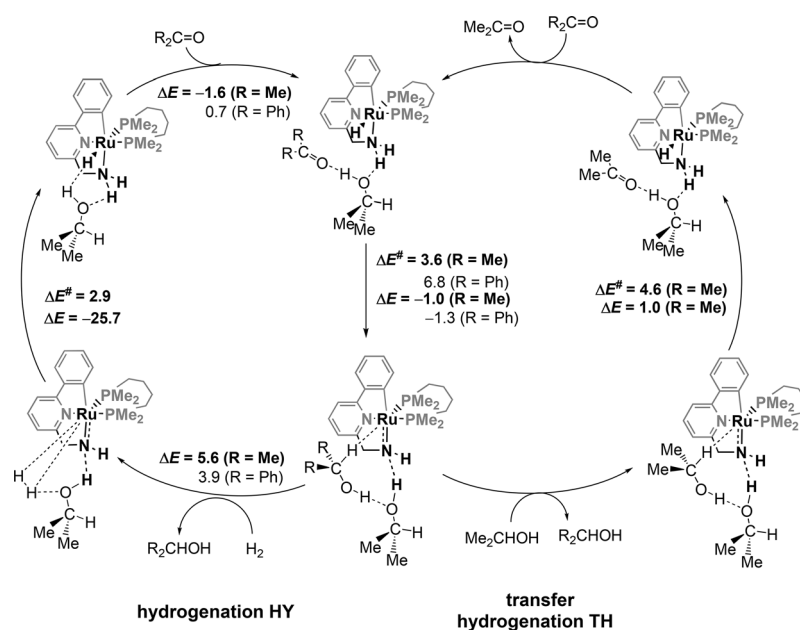**These are not the final page numbers!** ↗↗

Figure 9. Catalytic cycle for the TH and HY of acetone and benzophenone in the presence of a solvent molecule (2-propanol) with the model ruthenium catalyst **2-H** (solvent corrected E values in kcal mol^{-1}).

At this point the catalytic hydride species may be generated by displacement of the alcohol product R_2CHOH with 2-propanol (right cycle, TH) or by dihydrogen (left cycle, HY), according to Figures 7 and 8, respectively. The differences of the energy barriers between the two processes are very small. Transfer hydrogenation is limited by the C—H activation ($\Delta E^{\neq} = 4.6$ kcal mol^{-1}), whereas hydrogenation is controlled by H_2 activation ($\Delta E^{\neq} = 2.9$ kcal mol^{-1}), leading in both cases to the hydride complex. Notably, under the catalytic conditions, the Ru alkoxides are the predominant species (see previous NMR spectroscopic studies, Scheme 5), which quickly equilibrate to the hydride and the other catalytic intermediates. The energy differences between the intermediate species connected by the transition states are very small, in agreement with the high catalytic activity of the system. The energies for the substitution of acetone by the R_2CO substrate and R_2CHOH by 2-propanol are not given and depend on the R substituents. Similar views on the TH and HY mechanisms were reported by other authors.[57] Notably, the catalytic HY of ketones with the pincer **1-Cl** occurs in a defined "pH window" (Figure 6): Under acidic conditions, the Ru—H would be protonated resulting in H_2 formation, whereas in basic conditions the presence of a large amount of alkoxide would prevent H_2 coordination to the Ru center. By contrast, TH takes place under basic conditions and the catalytic activity increases with the alkoxide concentration reaching a "plateau".[40b]

Conclusion

We have reported the characterization and behavior of pincer alkoxide Ru complexes of the type [Ru(CNN)(OR)(dppb)] (R = Et (**1-OEt**) and CH_2CF_3 (**1-OCH$_2$CF$_3$**)) displaying the NH_2 function. A neutron diffraction experiment on the derivative **1-OCH$_2$CF$_3$**,

containing an alkoxide with a strong electron-withdrawing group, revealed a RuO···HN intramolecular hydrogen bond interaction. Conversely, NMR spectroscopic studies show that the solvated alkoxide **1-OEt·nEtOH** is labile in solution and leads to the hydride [RuH(CNN)(dppb)] (**1-H**) through: 1) Elimination of acetaldehyde and 2) reaction with H_2 through dihydrogen splitting. The solvent EtOH plays an active role in these processes, by increasing the lability of the Ru-alkoxide with respect to the EtO$^-$ ligand exchange and the formation of the hydride. The complex **1-Cl**, which is one of the most efficient transfer hydrogenation catalysts, shows high catalytic activity also in the hydrogenation of ketones to alcohols at a catalyst loading of 0.01 mol%. DFT calculations show a flat profile for the reaction between the Ru-hydride and the ketone substrate, leading to the Ru-alcohol-amide complex, followed by the formation of the most stable Ru-alkoxide. This is in agreement with the fact that the Ru-hydride and Ru-alkoxide are the only species detected in solution by NMR spectroscopy. The alcohol bound to the amide complex facilitates the C—H activation to generate the Ru-hydride catalyst and the coordination and activation of H_2 through hydrogen bond-assisted proton transfer. We have shown that the explicit inclusion of one solvent molecule (2-propanol) in the model system opens new interpretations to the reaction mechanism for both TH and HY processes.

Experimental Section

General

All reactions were carried out under an argon atmosphere by using standard Schlenk techniques. The solvents were carefully dried by standard methods and distilled under argon before use. Compounds **1-Cl**[33a] and **1'-Cl**[33d] were prepared according to literature procedures, whereas all other chemicals were purchased from Aldrich and Strem and used without further purification. NMR measurements were recorded on a Bruker AC 200 and Bruker Avance 500 spectrometer equipped with triple axis gradient apparatus. Chemical shifts (in ppm) are relative to TMS for ^{1}H and ^{13}C{^{1}H}, to CFCl$_3$ for ^{19}F{^{1}H}, whereas 85% H_3PO_4 was used for ^{31}P{^{1}H}. Elemental analyses (C, H, N) were carried out with a Carlo Erba 1106 elemental analyzer, whereas the GC analyses were performed with a Varian CP-3380 gas chromatograph.

↖↖ These are not the final page numbers!

Syntheses

[Ru(CNN)(OCH₂CF₃)(dppb)] **(1-OCH₂CF₃):** 2,2,2-Trifluoroethanol (30 mg, 0.30 mmol) was added to a 0.25 M solution of NaOEt (530 μL, 0.133 mmol) in ethanol, and the solvent was eliminated under reduced pressure, obtaining NaOCH₂CF₃. The complex **1-Cl** (95 mg, 0.125 mmol) and toluene (3.0 mL) were added and the suspension was stirred at room temperature for 2 h. The resulting orange-red solution was kept at −20 °C overnight, affording the precipitation of NaCl, and then filtered on Celite. The solution was concentrated (1 mL) and addition of pentane (3 mL) afforded a red precipitate, which was filtered, washed with pentane, and dried under reduced pressure. Yield: 96 mg (93 %). ^{1}H NMR (200.1 MHz, [D₆]benzene, 20 °C): $\delta = 8.25$ (t, $J(H,H) = 7.8$ Hz, 2 H; aromatic protons), 7.99 (t, $J(H,H) = 7.8$ Hz, 2 H; aromatic protons), 7.89 (s, 1 H; aromatic proton), 7.40–7.03 (m, 13 H; aromatic protons), 6.92 (d, $J(H,H) = 8.0$ Hz, 1 H; aromatic proton), 6.64 (m, 3 H; aromatic protons), 6.50 (t, $J(H,H) = 6.2$ Hz, 2 H; aromatic protons), 6.04 (m, 2 H; aromatic protons), 4.36 (br s, 1 H; NH₂), 3.87 (quintet, $J(H,H) = J_{HF} = 10.5$ Hz, 1 H; OCH₂), 3.31–2.89 (m, 5 H; OCH₂, CH₂P, CH₂N), 2.32 (s, 3 H; CH₃), 2.15–0.96 ppm (m, 7 H; CH₂P, NH₂); ^{13}C{^{1}H} NMR (50.3 MHz, [D₆]benzene, 20 °C): $\delta = 186.4$ (dd, $J_{CP} = 15.2, 8.5$ Hz; CRu), 163.7 (s; NCC), 157.2 (s; NCCH₂), 149.2–115.1 (m; aromatic carbons, CF₃), 65.0 (quartet, $J_{CF} = 29.7$ Hz; CH₂O), 52.1 (d, $J_{CP} = 2.5$ Hz; CH₂N), 31.3 (d, $J_{CP} = 24.6$ Hz; CH₂P), 30.9 (d, $J_{CP} = 29.1$ Hz; CH₂P), 26.9 (s; CH₂CH₂), 22.2 (s; CH₂CH₂), 22.1 ppm (s; CH₃); ^{31}P{^{1}H} NMR (81.0 MHz, [D₆]benzene, 20 °C): $\delta = 57.3$ (d, $^2J(P,P) = 35.5$ Hz), 39.6 ppm (d, $^2J(P,P) = 35.5$ Hz); ^{19}F{^{1}H} NMR (188.3 MHz, [D₆]benzene, 20 °C): $\delta = -76.7$ ppm; elemental analysis calcd (%) for C₄₃H₄₃F₃N₂OP₂Ru: C 62.69, H 5.26, N 3.40; found: C 62.83, H 5.35, N 3.29.

Treatment of 1-Cl with NaOEt in the presence of EtOH: A 0.25 M solution of NaOEt (230 μL, 0.058 mmol) in EtOH was dried under reduced pressure at room temperature for 30 min. Complex **1-Cl** (30 mg, 0.039 mmol), [D₆]benzene, (1.0 mL) and EtOH (3–25 equivalents) were added to NaOEt and the suspension was stirred at room temperature for 2 h, affording an orange solution that was transferred into a Wilmad quick pressure valve NMR tube and kept under argon or H₂ (5 atm). **1-OEt·nEtOH**: ^{1}H NMR (200.1 MHz, [D₆]benzene, 20 °C): $\delta = 8.10$ (m, 2 H; ortho-Ar-H), 7.90 (s, 1 H; Ar-H), 7.82 (t, $J(H,H) = 7.8$ Hz, 2 H; ortho-Ar-H), 7.41 (t, $J(H,H) = 7.4$ Hz, 2 H; meta-Ar-H), 7.31 (d, $J(H,H) = 7.8$ Hz, 1 H; Ar-H), 7.28 (m, 2 H; ortho-Ar-H), 7.19 (t, $J(H,H) = 7.4$ Hz, 1 H; para-Ar-H), 7.13 (m, 1 H; para-Ar-H), 7.08–7.03 (m, 5 H; Ar-H), 6.93 (d, $J(H,H) = 7.8$ Hz, 1 H; Ar-H), 6.83 (d, $J(H,H) = 8.0$ Hz, 1 H; Py-H), 6.78 (t, $J(H,H) = 7.9$ Hz, 1 H; Py-H), 6.68 (t, $J(H,H) = 7.3$ Hz, 1 H; para-Ar-H), 6.50 (t, $J(H,H) = 7.3$ Hz, 2 H; meta-Ar-H), 6.32 (d, $J(H,H) = 7.3$ Hz, 1 H; Py-H), 6.05 (t, $J(H,H) = 8.0$ Hz, 2 H; ortho-Ar-H), 3.93 (d, $J(H,H) = 14.0$ Hz, 1 H; NCH₂), 3.60 (m, 1 H; NH), 3.54 (s; HO of EtOH), 3.41 (q, $J(H,H) = 7.0$ Hz; CH₂O of EtOH), 3.34 (m, 1 H; NCH₂), 3.00 (pseudo t, $J(H,H)$ and $J(H,P) = 13.2$ Hz, 1 H; PCH₂), 2.76 (m, 1 H; PCH₂), 2.33 (s, 3 H; CH₃), 2.29 (m, 1 H; PCH₂), 2.01 (t, $J(H,H)$ and $J(H,P) = 14.2$ Hz, 1 H; PCH₂), 1.85 (s, 1 H; NH), 1.70–1.63 (m, 2 H; CH₂CH₂), 1.08 (t, $J(H,H) = 7.0$ Hz; CH₃CH₂ of EtOH), 0.95 ppm (m, 2 H; CH₂CH₂); ^{31}P{^{1}H} NMR (81.0 MHz, [D₆]benzene, 20 °C): $\delta = 54.7$ (d, $^2J(P,P) = 34.5$ Hz), 44.5 ppm (d, $^2J(P,P) = 34.5$ Hz).

General procedure for the catalytic HY of ketones: Complex **1-Cl** (1.3 mg, 1.7 μmol) was dissolved in EtOH (2 mL) under Ar. The ketone (4.3 mmol), the base KOtBu (9.6 mg, 0.086 mmol), and the solution containing the complex **1** (0.5 mL, 0.43 μmol) were added to EtOH (final volume 8.6 mL). The resulting solution was transferred into a thermostated reactor at 40 °C. The reduction was performed by introducing dihydrogen at a pressure of 5 atm and the

conversion was determined by GC analysis (**1**, 0.01 mol %, KOtBu 2 mol %, ketone 0.5 M).

Single-crystal X-ray structure determination: 1-OCH₂CF₃·1.5 ([D₆]benzene)

Formula: C₄₃H₄₃F₃N₂OP₂Ru·1.5([D₆]benzene); $M_r = 949.98$; crystal color and shape: red-brown fragment, crystal dimensions: $0.33 \times 0.36 \times 0.43$ mm; crystal system: monoclinic; space group $P2_1/n$ (no. 14); $a = 10.7773(4)$, $b = 13.6967(4)$, $c = 30.6054(13)$ Å; $\beta = 90.557(3)°$; $V = 4517.6(3)$ Å³; $Z = 4$; $\mu(Mo_{K\alpha}) = 0.471$ mm⁻¹; $\rho_{calcd} = 1.397$ g cm⁻³; θ range = 2.97–25.34°; data collected: 38060; independent data [$I_o > 2\sigma(I_o)$/all data/R_{int}]: 6612/8233/0.047; data/restraints/parameters: 8233/0/551; R1 [$I_o > 2\sigma(I_o)$/all data]: 0.0296/0.0408; wR2 [$I_o > 2\sigma(I_o)$/all data]: 0.0697/0.0719; GOF = 0.968; $\Delta\rho_{max/min}$: 0.90/−0.54 e Å⁻³.

Single-crystal neutron structure determination of compound 1-OCH₂CF₃·1.5 ([D₆]benzene)

Formula: C₄₃H₄₃F₃N₂OP₂Ru·1.5([D₆]benzene); $M_r = 949.98$; crystal color and shape: red-brown fragment, crystal dimensions: several mm³; crystal system: monoclinic; space group $P2_1/n$ (no. 14); $a = 10.7452(3)$, $b = 13.5800(3)$, $c = 30.4453(7)$ Å; $\beta = 90.7550(9)°$; $V = 4442.19(19)$ Å³; $Z = 4$; $\rho_{calcd} = 1.421$ g cm⁻³; θ range = 3.37–54.13°; data collected: 28526; independent data [$I_o > 2\sigma(I_o)$/all data/R_{int}]: 5435/6310/0.059; data/restraints/parameters: 6310/0/1018; R1 [$I_o > 2\sigma(I_o)$/all data]: 0.0460/0.0596; wR2 [$I_o > 2\sigma(I_o)$/all data]: 0.0885/0.0947; GOF = 1.115; $\Delta\rho_{max/min}$: 0.64/−0.66 fm Å⁻³. The neutron diffraction experiment was conducted at 20.0(5) K using a wavelength of 1.4587 Å, at the Institut Laue-Langevin, Grenoble, using the monochromatic thermal neutron diffractometer D19 equipped with the new horizontally curved "banana-shaped" very large 120 × 30° position sensitive detector.

Crystallographic data (excluding structure factors) for the structures reported in this paper have been deposited with the Cambridge Crystallographic Data Centre as supplementary publication no. CCDC-872929 (Neutron) and CCDC-872930 (X-ray). These data can be obtained free of charge from The Cambridge Crystallographic Data Centre via www.ccdc.cam.ac.uk/data_request/cif. For more details, see Supporting Information.

Computational details

All calculations were performed using the Gaussian 03 software package,[58] and the PBE0 functional, without symmetry constraints. That functional uses a hybrid generalized gradient approximation (GGA), including 25 % mixture of Hartree–Fock[59] exchange with DFT[60] exchange-correlation, given by the PBE functional.[61] The optimized geometries were obtained with a LanL2DZ basis set[62] augmented with a f-polarization function[63] for Ru and with one d-polarization function for P,[64] and a standard 6–31G(d,p)[65] for the remaining elements (basis b1). Transition state optimizations were performed with the Synchronous Transit-Guided Quasi-Newton Method (STQN).[66] Frequency calculations were performed to confirm the nature of the stationary points. Transition states were confirmed by following their vibrational modes downhill. The energy profiles reported result from single point energy calculations using an improved basis set (basis b2) and the geometries optimized at the PBE0/b1 level. Basis b2 consisted of the Stuttgart/Dresden ECP (SDD) basis set[67] with an added f-polarization function for Ru,[63] and standard 6–311++G(d,p)[68] for the remaining elements. Solvent effects (2-propanol) were considered in the PBE0/b2//PBE0/b1 energy calculations by using the polarizable continuum model

These are not the final page numbers! ↗↗

Acknowledgements

[1] a) G. Shang, W. Li, X. Zhang, *Catalytic Asymmetric Synthesis*, 3edrd ed(Ed.: I. Ojima), John Wiley & Sons, Hoboken, **2010**; Chapter 7; b) *The Handbook of Homogeneous Hydrogenation, Vols. 1–3* (Eds. J. G. de Vries, C. J. Elsevier), Wiley-VCH, Weinheim, **2007**; c) *Transition Metals for Organic Synthesis*, 2edndd ed(Eds.: M. Beller, C. Bolm), Wiley-VCH, Weinheim, **2004**, p. 29; d) *Asymmetric Catalysis on Industrial Scale* (Eds.: H.-U. Blaser, E. Schmidt), Wiley-VCH, Weinheim, **2004**.

[2] a) R. H. Morris, *Chem. Soc. Rev.* **2009**, *38*, 2282; b) W. Baratta, P. Rigo, *Eur. J. Inorg. Chem.* **2008**, 4041; c) C. Wang, X. Wu, J. Xiao, *Chem. Asian J.* **2008**, *3*, 1750; d) D. J. Morris, M. Wills, *Chim. Oggi* **2007**, *25*, 11; e) T. Ikar-iya, A. J. Blacker, *Acc. Chem. Res.* **2007**, *40*, 1300; f) J. S. M. Samec, J. E. Bäckvall, P. G. Andersson, P. Brandt, *Chem. Soc. Rev.* **2006**, *35*, 237; g) S. Gladiali, E. Alberico, *Chem. Soc. Rev.* **2006**, *35*, 226; h) T. Ikariya, K. Murata, R. Noyori, *Org. Biomol. Chem.* **2006**, *4*, 393.

[3] a) W. Baratta, M. Ballico, A. Del Zotto, K. Siega, S. Magnolia, P. Rigo, *Chem. Eur. J.* **2008**, *14*, 2557; b) W. Baratta, C. Barbato, S. Magnolia, K. Siega, P. Rigo, *Chem. Eur. J.* **2010**, *16*, 3201.

[4] Primary alcohols, such as ethanol or methanol, are generally less suitable hydrogen donors, due to their unfavorable redox potential, see: H. Adkins, R. M. Elofson, A. G. Rossow, C. C. Robinson, *J. Am. Chem. Soc.* **1949**, *71*, 3622.

[5] a) T. C. Johnson, D. J. Morris, M. Wills, *Chem. Soc. Rev.* **2010**, *39*, 81; b) G. E. Dobereiner, R. H. Crabtree, *Chem. Rev.* **2010**, *110*, 681; c) B. Loges, H. Junge, B. Spilker, C. Fischer, M. Beller, *Chem.-Ing.-Tech.* **2007**, *79*, 741; d) M. H. S. A. Hamid, P. A. Slatford, J. M. J. Williams, *Adv. Synth. Catal.* **2007**, *349*, 1555.

[6] a) S. E. Clapham, A. Hadzovic, R. H. Morris, *Coord. Chem. Rev.* **2004**, *248*, 2201; b) P. Espinet, A. C. Albéniz, *Fundamentals of Molecular Catalysis, Current Methods in Inorganic Chemistry, Vol. 3* (Eds.: H. Kurosawa, A. Ya-mamoto), Elsevier, Amsterdam, **2003**, Chapter 6, p. 328; c) *Recent Advances in Hydride Chemistry* (Eds.: M. Peruzzini, R. Poli), Elsevier, Amsterdam, **2001**.

[7] a) D. C. Bradley, R. C. Mehrotra, I. P. Rothwell, A. Singh, *Alkoxo and Aryloxo Derivatives of Metals*, Academic Press, New York, **2001**; b) J. R. Fulton, A. W. Holland, D. J. Fox, R. G. Bergman, *Acc. Chem. Res.* **2002**, *35*, 44; c) H. E. Bryndza, W. Tam, *Chem. Rev.* **1988**, *88*, 1163.

[8] G. J. Kubas, *Chem. Rev.* **2007**, *107*, 4152.

[9] a) H. E. Bryndza, J. C. Calabrese, M. Marsi, D. C. Roe, W. Tam, J. E. Bercaw, *J. Am. Chem. Soc.* **1986**, *108*, 4805; b) H. Itagaki, N. Koga, K. Morokuma, Y. Saito, *Organometallics* **1993**, *12*, 1648.

[10] O. Blum, D. Milstein, *J. Organomet. Chem.* **2000**, *593*, 479.

[11] K. J. Haack, S. Hashiguchi, A. Fujii, T. Ikariya, R. Noyori, *Angew. Chem.* **1997**, *109*, 297; *Angew. Chem. Int. Ed. Engl.* **1997**, *36*, 285.

[12] H. Doucet, T. Ohkuma, K. Murata, T. Yokozawa, M. Kozawa, E. Katayama, A. F. England, T. Ikariya, R. Noyori, *Angew. Chem.* **1998**, *110*, 1792; *Angew. Chem. Int. Ed.* **1998**, *37*, 1703.

[13] BINAP = (1,1'-binaphthalene)-2,2'-diylbis(1,1-diphenylphosphane).

[14] a) M. Yamakawa, H. Ito, R. Noyori, *J. Am. Chem. Soc.* **2000**, *122*, 1466; b) D. G. I. Petra, J. N. H. Reek, J. W. Handgraaf, E. J. Meijer, P. Dierkes, P. C. J. Kamer, J. Brussee, H. E. Schoemaker, P. W. N. M. van Leeuwen, *Chem. Eur. J.* **2000**, *6*, 2818; c) B. G. Zhao, Z. B. Han, K. L. Ding, *Angew. Chem.* **2013**, *125*, 4844; *Angew. Chem. Int. Ed.* **2013**, *52*, 4744.

[15] T. Koike, T. Ikariya, *Organometallics* **2005**, *24*, 724.

[16] D. A. Alonso, P. Brandt, S. J. M. Nordin, P. G. Andersson, *J. Am. Chem. Soc.* **1999**, *121*, 9580.

[17] C. A. Sandoval, T. Ohkuma, K. Muniz, R. Noyori, *J. Am. Chem. Soc.* **2003**, *125*, 13490.

[18] K. Abdur-Rashid, S. E. Clapham, A. Hadzovic, J. N. Harvey, A. J. Lough, R. H. Morris, *J. Am. Chem. Soc.* **2002**, *124*, 15104.

[19] a) K. Abdur-Rashid, M. Faatz, A. J. Lough, R. H. Morris, *J. Am. Chem. Soc.* **2001**, *123*, 7473; b) T. Li, R. Churlaud, A. J. Lough, K. Abdur-Rashid, R. H. Morris, *Organometallics* **2004**, *23*, 6239.

[20] a) J. M. John, S. Takebayashi, N. Dabral, M. Miskolzie, S. H. Bergens, *J. Am. Chem. Soc.* **2013**, *135*, 8578; b) R. J. Hamilton, S. H. Bergens, *J. Am. Chem. Soc.* **2008**, *130*, 11979; c) R. J. Hamilton, S. H. Bergens, *J. Am. Chem. Soc.* **2006**, *128*, 13700.

[21] S. Takebayashi, N. Dabral, M. Miskolzie, S. H. Bergens, *J. Am. Chem. Soc.* **2011**, *133*, 9666.

[22] C. A. Sandoval, Y. Yamaguchi, T. Ohkuma, K. Kato, R. Noyori, *Magn. Reson. Chem.* **2006**, *44*, 66.

[23] R. J. Hamilton, C. G. Leong, G. Bigam, M. Miskolzie, S. H. Bergens, *J. Am. Chem. Soc.* **2005**, *127*, 4152.

[24] M. Ito, M. Hirakawa, K. Murata, T. Ikariya, *Organometallics* **2001**, *20*, 379.

[25] C. Hedberg, K. Källström, P. I. Arvidsson, P. Brandt, P. G. Andersson, *J. Am. Chem. Soc.* **2005**, *127*, 15083.

[26] a) W. Baratta, E. Herdtweck, K. Siega, M. Toniutti, P. Rigo, *Organometallics* **2005**, *24*, 1660; b) W. Baratta, G. Chelucci, E. Herdtweck, S. Magnolia, K. Siega, P. Rigo, *Angew. Chem.* **2007**, *119*, 7795; *Angew. Chem. Int. Ed.* **2007**, *46*, 7651; c) T. Ohkuma, C. A. Sandoval, R. Srinivasan, Q. Lin, Y. Wei, K. Muñiz, R. Noyori, *J. Am. Chem. Soc.* **2005**, *127*, 8288; d) C. A. Sandoval, Y. Li, K. Ding, R. Noyori, *Chem. Asian J.* **2008**, *3*, 1801; e) S. Zhang, S. Baldino, W. Baratta, *Organometallics* **2013**, *32*, 5299.

[27] a) T. Ohkuma, N. Utsumi, K. Tsutsumi, K. Murata, C. Sandoval, R. Noyori, *J. Am. Chem. Soc.* **2006**, *128*, 8724; b) T. Ohkuma, K. Tsutsumi, N. Utsumi, N. Arai, R. Noyori, K. Murata, *Org. Lett.* **2007**, *9*, 255.

[28] A. Hadzovic, D. Song, C. M. MacLaughlin, R. H. Morris, *Organometallics* **2007**, *26*, 5987.

[29] E. Putignano, G. Bossi, P. Rigo, W. Baratta, *Organometallics* **2012**, *31*, 1133.

[30] a) N. D. Schley, G. E. Dobereiner, R. H. Crabtree, *Organometallics* **2011**, *30*, 4174; b) A. Nova, D. Balcells, N. D. Schley, G. E. Dobereiner, R. H. Crabtree, O. Eisenstein, *Organometallics* **2010**, *29*, 6548.

[31] A. Comas-Vives, G. Ujaque, A. Lledos, *Adv. Inorg. Chem.* **2010**, *62*, 231.

[32] W. N. O. Wylie, A. J. Lough, R. H. Morris, *Organometallics* **2011**, *30*, 1236.

[33] a) W. Baratta, G. Chelucci, S. Gladiali, K. Siega, M. Toniutti, M. Zanette, E. Zangrando, P. Rigo, *Angew. Chem.* **2005**, *117*, 6370; *Angew. Chem. Int. Ed.* **2005**, *44*, 6214; b) W. Baratta, M. Bosco, G. Chelucci, A. Del Zotto, K. Siega, M. Toniutti, E. Zangrando, P. Rigo, *Organometallics* **2006**, *25*, 4611; c) W. Baratta, K. Siega, P. Rigo, *Adv. Synth. Catal.* **2007**, *349*, 1633; d) W. Baratta, G. Chelucci, S. Magnolia, K. Siega, P. Rigo, *Chem. Eur. J.* **2009**, *15*, 726; e) S. Zhang, W. Baratta, *Organometallics* **2013**, *32*, 3339.

[34] a) W. Baratta, M. Ballico, G. Chelucci, K. Siega, P. Rigo, *Angew. Chem.* **2008**, *120*, 4434; *Angew. Chem. Int. Ed.* **2008**, *47*, 4362; b) W. Baratta, M. Ballico, S. Baldino, G. Chelucci, E. Herdtweck, K. Siega, S. Magnolia, P. Rigo, *Chem. Eur. J.* **2008**, *14*, 9148; c) W. Baratta, F. Benedetti, A. Del Zotto, L. Fanfoni, F. Felluga, S. Magnolia, E. Putignano, P. Rigo, *Organometallics* **2010**, *29*, 3563.

[35] W. Baratta, L. Fanfoni, S. Magnolia, K. Siega, P. Rigo, *Eur. J. Inorg. Chem.* **2010**, 1419.

[36] W. Baratta, G. Bossi, E. Putignano, P. Rigo, *Chem. Eur. J.* **2011**, *17*, 3474.

[37] a) M. Nielsen, A. Kammer, D. Cozzula, H. Junge, S. Gladiali, M. Beller, *Angew. Chem. Int. Ed.* **2011**, *50*, 9563; b) M. Nielsen, H. Junge, A. Kammer, M. Beller, *Angew. Chem.* **2012**, *124*, 5809; *Angew. Chem. Int. Ed.* **2012**, *51*, 5711.

[38] S. Agrawal, M. Lenormand, B. Martín-Matute, *Org. Lett.* **2012**, *14*, 1456.

[39] G. Bossi, E. Putignano, P. Rigo, W. Baratta, *Dalton Trans.* **2011**, *40*, 8986.

[40] a) W. Baratta, M. Ballico, G. Esposito, P. Rigo, *Chem. Eur. J.* **2008**, *14*, 5588; b) W. Baratta, K. Siega, P. Rigo, *Chem. Eur. J.* **2007**, *13*, 7479.

[41] a) D. M. Hoffman, D. Lappas, D. A. Wierda, *J. Am. Chem. Soc.* **1989**, *111*, 1531; b) D. M. Hoffman, D. Lappas, D. A. Wierda, *J. Am. Chem. Soc.* **1993**, *115*, 10538.

[42] M. Bertoli, A. Choualeb, A. J. Lough, B. Moore, D. Spasyuk, D. G. Gusev, *Organometallics* **2011**, *30*, 3479.

[43] For isolated Ru-OCH$_2$CF$_3$ complexes see: a) T. J. Johnson, J. C. Huffman, K. G. Caulton, *J. Am. Chem. Soc.* **1992**, *114*, 2725; b) T. J. Johnson, K. Folting, W. E. Streib, J. D. Martin, J. C. Huffman, S. A. Jackson, O. Eisenstein, K. G. Caulton, *Inorg. Chem.* **1995**, *34*, 488. For Ru complexes containing bidentate alkoxide-amino ligands, see: c) M. Hennig, K. Puntener, M. Scalone, *Tetrahedron: Asymmetry* **2000**, *11*, 1849; d) K. Everaere, A. Mortreux, M. Bulliard, J. Brussee, A. van der Gen, G. Nowogrocki, J.-F. Carpentier, *Eur. J. Org. Chem.* **2001**, 275.

[44] a) T. Steiner, *Angew. Chem.* **2002**, *114*, 50; *Angew. Chem. Int. Ed.* **2002**, *41*, 48; b) L. Brammer, *Dalton Trans.* **2003**, 3145; c) G. Aullón, D. Bellamy, L. Brammer, E. A. Bruton, A. G. Orpen, *Chem. Commun.* **1998**, 653.

[45] W. Baratta, M. Ballico, A. Del Zotto, E. Herdtweck, S. Magnolia, R. Peloso, K. Siega, M. Toniutti, E. Zangrando, P. Rigo, *Organometallics* **2009**, *28*, 4421.

[46] Y. H. Lai, T. Y. Chou, Y. H. Song, C. S. Liu, Y. Chi, A. J. Carty, S. M. Peng, G. H. Lee, *Chem. Mater.* **2003**, *15*, 2454.

[47] S. E. Clapham, R. Guo, M. Zimmer-De Iuliis, N. Rasool, A. J. Lough, R. H. Morris, *Organometallics* **2006**, *25*, 5477.

[48] The formation of acetaldehyde ($\delta = 9.85$ and 1.42 ppm in [D$_6$]benzene) was observed through a ^{1}H-^{1}H TOCSY experiment.

[49] a) S. E. Shubina, N. V. Belkova, A. N. Krylov, E. V. Vorontsov, L. M. Epstein, D. G. Gusev, M. Niedermann, H. Berke, *J. Am. Chem. Soc.* **1996**, *118*, 1105; b) D. Donghi, T. Beringhelli, G. D'Alfonso, M. Mondini, *Chem. Eur. J.* **2006**, *12*, 1016.

[50] In addition to the hydride at $\delta = -7.17$ ppm, we also observed the presence of another hydride at $\delta = -9.50$ ppm. This resonance does not show any exchange NOESY cross-peaks with molecular hydrogen or with the other hydride complexes at RT, and there is no CSA-DD distortion pattern thus it is likely to be an off-pathway species.

[51] Turnover frequency (moles of ketone converted to alcohol per mole of catalyst per hour) at 50% conversion.

[52] J. W. Handgraaf, E. J. Meijer, *J. Am. Chem. Soc.* **2007**, *129*, 3099.

[53] P. A. Dub, T. Ikariya, *J. Am. Chem. Soc.* **2013**, *135*, 2604.

[54] a) S. Aime, E. Diana, R. Gobetto, M. Milanesio, E. Valls, D. Viterbo, *Organometallics* **2002**, *21*, 50; b) N. V. Belkova, E. S. Shubina, E. I. Gustul, L. M. Epstein, I. L. Eremenko, S. E. Nefedov, *J. Organomet. Chem.* **2000**, *610*, 58; c) J. Wessel, J. C. Lee Junior, E. Peris, G. P. A. Yap, J. B. Fortin, J. S. Ricci, G. Sini, A. Albinati, T. F. Koetzle, O. Eisenstein, A. L. Rheingold, R. H. Crabtree, *Angew. Chem.* **1995**, *107*, 2711; *Angew. Chem. Int. Ed. Engl.* **1995**, *34*, 2507.

[55] a) N. V. Belkova, E. S. Shubina, L. M. Epstein, *Acc. Chem. Res.* **2005**, *38*, 624; b) N. V. Belkova, E. Collange, P. Dub, L. M. Epstein, D. A. Lemenovskii, A. Lledós, O. Maresca, F. Maseras, R. Poli, P. O. Revin, E. S. Shubina, E. V. Vorontsov, *Chem. Eur. J.* **2005**, *11*, 873; c) N. V. Belkova, M. Besora, M. Baya, P. Dub, L. M. Epstein, A. Lledós, R. Poli, P. O. Revin, E. S. Shubina, *Chem. Eur. J.* **2008**, *14*, 9921; d) P. Dub, N. V. Belkova, O. A. Filipov, J.-C. Daran, L. M. Epstein, A. Lledós, E. S. Shubina, R. Poli, *Chem. Eur. J.* **2010**, *16*, 189; e) P. Dub, O. A. Filipov, N. V. Belkova, J.-C. Daran, L. M. Epstein, R. Poli, E. S. Shubina, *Dalton Trans.* **2010**, *39*, 2008; f) A. Ienco, M. J. Calhorda, J. Reinhold, F. Reineri, C. Bianchini, M. Peruzzini, F. Vizza, C. Mealli, *J. Am. Chem. Soc.* **2004**, *126*, 11954.

[56] A. Rossin, G. Kovács, G. Ujaque, A. Lledós, F. Joó, *Organometallics* **2006**, *25*, 5010.

[57] X. Zhang, X. Guo, Y. Chen, Y. Tang, M. Lei, W. Fang, *Phys. Chem. Chem. Phys.* **2012**, *14*, 6003.

[58] Gaussian 03, Revision C.02, M. J. Frisch, G. W. Trucks, H. B. Schlegel, G. E. Scuseria, M. A. Robb, J. R. Cheeseman, J. A. Montgomery, Jr., T. Vreven, K. N. Kudin, J. C. Burant, J. M. Millam, S. S. Iyengar, J. Tomasi, V. Barone, B. Mennucci, M. Cossi, G. Scalmani, N. Rega, G. A. Petersson, H. Nakatsuji, M. Hada, M. Ehara, K. Toyota, R. Fukuda, J. Hasegawa, M. Ishida, T. Nakajima, Y. Honda, O. Kitao, H. Nakai, M. Klene, X. Li, J. E. Knox, H. P. Hratchian, J. B. Cross, C. Adamo, J. Jaramillo, R. Gomperts, R. E. Stratmann, O. Yazyev, A. J. Austin, R. Cammi, C. Pomelli, J. W. Ochterski, P. Y. Ayala, K. Morokuma, G. A. Voth, P. Salvador, J. J. Dannenberg, V. G. Zakrzewski, S. Dapprich, A. D. Daniels, M. C. Strain, O. Farkas, D. K. Malick, A. D. Rabuck, K. Raghavachari, J. B. Foresman, J. V. Ortiz, Q. Cui, A. G. Baboul, S. Clifford, J. Cioslowski, B. B. Stefanov, G. Liu, A. Liashenko, P. Piskorz, I. Komaromi, R. L. Martin, D. J. Fox, T. Keith, M. A. Al-Laham, C. Y. Peng, A. Nanayakkara, M. Challacombe, P. M. W. Gill, B. Johnson, W. Chen, M. W. Wong, C. Gonzalez, J. A. Pople, Gaussian, Inc., Wallingford CT, **2004**.

[59] W. J. Hehre, L. Radom, P. v. R. Schleyer, J. A. Pople, *Ab Initio Molecular Orbital Theory*, John Wiley & Sons, New York, **1986**.

[60] R. G. Parr, W. Yang, *Density Functional Theory of Atoms and Molecules*, Oxford University Press, New York, **1989**.

[61] a) J. P. Perdew, K. Burke, M. Ernzerhof, *Phys. Rev. Lett.* **1997**, *78*, 1396; b) J. P. Perdew, *Phys. Rev. B* **1986**, *33*, 8822.

[62] a) T. H. Dunning Jr., P. J. Hay, *Modern Theoretical Chemistry, Vol. 3* (Ed.: H. F. Schaefer, III), Plenum, New York, **1976**, p.1; b) P. J. Hay, W. R. Wadt, *J. Chem. Phys.* **1985**, *82*, 270; c) W. R. Wadt, P. J. Hay, *J. Chem. Phys.* **1985**, *82*, 284; d) P. J. Hay, W. R. Wadt, *J. Chem. Phys.* **1985**, *82*, 2299.

[63] A. W. Ehlers, M. Böhme, S. Dapprich, A. Gobbi, A. Höllwarth, V. Jonas, K. F. Köhler, R. Stegmann, A. Veldkamp, G. Frenking, *Chem. Phys. Lett.* **1993**, *208*, 111.

[64] A. Höllwarth, M. Böhme, S. Dapprich, A. W. Ehlers, A. Gobbi, V. Jonas, K. F. Köhler, R. Stegmann, A. Veldkamp, G. Frenking, *Chem. Phys. Lett.* **1993**, *208*, 237.

[65] a) R. Ditchfield, W. J. Hehre, J. A. Pople, *J. Chem. Phys.* **1971**, *54*, 724; b) W. J. Hehre, R. Ditchfield, J. A. Pople, *J. Chem. Phys.* **1972**, *56*, 2257; c) P. C. Hariharan, J. A. Pople, *Mol. Phys.* **1974**, *27*, 209; d) M. S. Gordon, *Chem. Phys. Lett.* **1980**, *76*, 163; e) P. C. Hariharan, J. A. Pople, *Theor. Chim. Acta* **1973**, *28*, 213.

[66] a) C. Peng, P. Y. Ayala, H. B. Schlegel, M. J. Frisch, *J. Comput. Chem.* **1996**, *17*, 49; b) C. Peng, H. B. Schlegel, *Isr. J. Chem.* **1993**, *33*, 449.

[67] a) U. Häusermann, M. Dolg, H. Stoll, H. Preuss, *Mol. Phys.* **1993**, *78*, 1211; b) W. Küchle, M. Dolg, H. Stoll, H. Preuss, *J. Chem. Phys.* **1994**, *100*, 7535; c) T. Leininger, A. Nicklass, H. Stoll, M. Dolg, P. Schwerdtfeger, *J. Chem. Phys.* **1996**, *105*, 1052.

[68] a) A. D. McLean, G. S. Chandler, *J. Chem. Phys.* **1980**, *72*, 5639; b) R. Krishnan, J. S. Binkley, R. Seeger, J. A. Pople, *J. Chem. Phys.* **1980**, *72*, 650; c) A. J. H. Wachters, *J. Chem. Phys.* **1970**, *52*, 1033; d) P. J. Hay, *J. Chem. Phys.* **1977**, *66*, 4377; e) K. Raghavachari, G. W. Trucks, *J. Chem. Phys.* **1989**, *91*, 1062; f) R. C. Binning Jr., L. A. Curtiss, *J. Comput. Chem.* **1990**, *11*, 1206; g) M. P. McGrath, L. Radom, *J. Chem. Phys.* **1991**, *94*, 511; h) T. Clark, J. Chandrasekhar, G. W. Spitznagel, P. v. R. Schleyer, *J. Comput. Chem.* **1983**, *4*, 294; i) M. J. Frisch, J. A. Pople, J. S. Binkley, *J. Chem. Phys.* **1984**, *80*, 3265.

[69] a) M. T. Cancès, B. Mennucci, J. Tomasi, *J. Chem. Phys.* **1997**, *107*, 3032; b) M. Cossi, V. Barone, B. Mennucci, J. Tomasi, *Chem. Phys. Lett.* **1998**, *286*, 253; c) B. Mennucci, J. Tomasi, *J. Chem. Phys.* **1997**, *106*, 5151.

[70] a) J. Tomasi, B. Mennucci, R. Cammi, *Chem. Rev.* **2005**, *105*, 2999; b) M. Cossi, G. Scalmani, N. Rega, V. Barone, *J. Chem. Phys.* **2002**, *117*, 43.
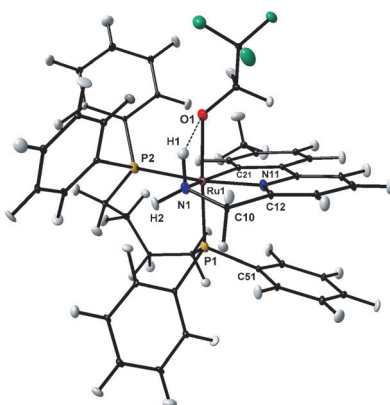
FULL PAPER

W. Baratta,* S. Baldino, M. J. Calhorda,
P. J. Costa, G. Esposito, E. Herdtweck,
S. Magnolia, C. Mealli, A. Messaoudi,
S. A. Mason, L. F. Veiros

■■ – ■■

CNN Pincer Ruthenium Catalysts for Hydrogenation and Transfer Hydrogenation of Ketones: Experimental and Computational Studies

Ru stabilized: Solid state and solution studies show that the catalytically active pincer alkoxide-amine ruthenium complexes are stabilized by hydrogen bonds (see figure) and reversibly give ruthenium hydride species by H elimination or H_2 splitting. DFT calculations show that the pincer alkoxides are the most stable complexes, which rapidly form from the ruthenium hydride and carbonyl compounds through a non-observable "amide" alcohol intermediate.

↖↖ These are not the final page numbers!